Version of Record: https://www.sciencedirect.com/science/article/pii/S0001870824000033
Manuscript_9c396af632a99a9ff8e1c94c90a36000

SYZ MIRROR SYMMETRY FOR DEL PEZZO SURFACES AND AFFINE STRUCTURES

SIU-CHEONG LAU, TSUNG-JU LEE, AND YU-SHEN LIN

Abstract. We prove that the Landau–Ginzburg superpotential of del Pezzo surfaces can be realized as a limit of their hyperKähler rotation toward the large complex structure limit point. As a corollary, we compute the limit of the complex affine structure of the special Lagrangian fibrations constructed by Collins–Jacob–Lin in $\mathbf{P}^1 \times \mathbf{P}^1$ [17] and compare it with the integral affine structures used in the work of Carl–Pumperla–Siebert [9]. We also construct the Floer-theoretical Landau–Ginzburg mirrors of smoothing of A_n-singularities and monotone del Pezzo surfaces, by using the gluing method of Cho–Hong–Lau [12] and Hong–Kim–Lau [40]. They agree with the result of limit of hyperKähler rotations.

Contents

1. Introduction

The Strominger–Yau–Zaslow conjecture [59] (SYZ conjecture) predicts that

(1) a Calabi–Yau manifold X near a large complex structure limit, where mirror symmetry is expected to happen, admits a special Lagrangian torus fibration;
(2) the mirror $\check{X}$ of X can be constructed from the dual torus fibration of X, with the complex structure receiving "quantum corrections" from the holomorphic discs with boundaries on the special Lagrangian torus fibres in X.

For the purpose of mirror symmetry, the goal is to understand how the quantum corrections affect the mirror construction.

However, the original conjecture is hard due to the difficulties from analysis: there is very little known about the behavior of the Calabi–Yau metrics. To construct the special

2010 *Mathematics Subject Classification.* Primary: 32Q25, 53D37. Secondary: 14J27, 14J33.

Lagrangian fibrations, one would need to first understand the Calabi–Yau metric. To understand the Calabi–Yau metric, the conjecture leads us to the study of holomorphic discs with boundaries on the special Lagrangian fibres. Thus, the problems of Calabi–Yau metrics, existence of special Lagrangian fibrations and quantum corrections from holomorphic discs are closely linked together.

To avoid the difficulties in analysis in the metric level and due to the interests from mirror symmetry, there are replacements for the original proposal from algebraic geometry and symplectic geometry. On the algebraic side, Kontsevich–Soibelman [45] and Gross–Siebert programs [31] introduced the notion of scattering diagrams for understanding the quantum correction. On the symplectic side, Fukaya proposed the family Floer homology [22] and later studied by Tu [62], Abouzaid [1–3], and Yuan [63]. There is another approach using relative symplectic cohomology [28]. Both approaches are designed to capture the quantum corrections in the mirror construction and both have big success in explaining mirror symmetry in an intrinsic way. However, it is still unclear how the two approaches are related to the original conjecture explicitly, again due to the lacking of the existence of genuine SYZ fibrations. Until very recently, T. Collins, A. Jacob, and the third author constructed the first non-trivial example[1] of genuine special Lagrangian fibrations [17]. In this paper, we will study the complex affine structures on the base of the genuine special Lagrangian fibrations in these examples and explain that there can be subtle differences between the SYZ bases and the affine manifold with singularities used in the Gross–Siebert program (in this case is worked out by Carl–Pumperla–Siebert), which is a long-termed folklore conjecture. We refer the readers to [29, Section 7] and [11, Section 1] and references therein.

Mirror symmetry has been extended to Fano manifolds [43]. In which case, the mirror of a Fano manifold Y is a Landau–Ginzburg superpotential W. The superpotential W is expected to recover the enumerative geometry of Y in various aspects. For instance, the quantum cohomology $\mathrm{QH}^*(Y)$ is isomorphic to the Jacobian ring $\mathrm{Jac}(W)$ [8, 23] and the quantum periods of W give the generating function of the descendant Gromov–Witten invariants [14, 15, 26, 41]. Recently it is proved that superpotential agrees with the open mirror map of the corresponding local Calabi–Yau threefold mirror symmetry in the case of toric del Pezzo surfaces [27]. Auroux–Katzarkov–Orlov [6] proved homological mirror symmetry, i.e., the Fukaya–Seidel category $FS(W)$ is A_∞-equivalent to the derived category of coherent sheaves $D^b\mathrm{Coh}(Y)$. In particular, they showed that the superpotential of a del Pezzo surface of degree d can be topologically compactified as a rational elliptic surface with an I_d fibre. Therefore, an important task is to derive the superpotential for a given Fano manifold. In the case of toric del Pezzo surfaces, the superpotential can be read off from the toric data [25, 42], which is the generating function of a weighted count of Maslov index two pseudo-holomorphic discs with boundary on SYZ fibres in Y [13]. The latter is called the Lagrangian Floer-theoretic potential of the moment fibres. A folklore conjecture is that the Lagrangian Floer-theoretic potentials of monotone Lagrangians in Y can be glued via the wall-crossing formula and one obtains the Landau–Ginzburg superpotential of Y.

[1]In the sense that a priori without knowing the existence of elliptic fibration structure after hyperKähler rotation, which is a technical part in analysis.

Let Y be a del Pezzo surface of degree d and $D \in |-K_Y|$ be a smooth anti-canonical divsior. There exists a meromorphic 2-form on Y with a simple pole on D unique up to $\mathbb{C}^*$-scaling and restrict to a nowhere vanishing holomorphic 2-form on $X = Y \setminus D$. Tian–Yau proved that X is equipped with an exact complete Calabi-Yau metric ω_{TY} such that $2\omega_{TY}^2 = \Omega \wedge \bar{\Omega}$ [61]. Throughout the paper, we will denote denote $\omega = \omega_{\mathrm{TY}}$ the exact Tian–Yau metric for simplicity. It is crucial to note that we will use the exact Tian–Yau metric. Responding to the SYZ conjecture [59] and conjectures of Auroux [5], Collins–Jacob–Lin proved that

Theorem 1.1 (cf. [17]). *There exists a special Lagrangian fibration $X \to B \cong \mathbb{R}^2$ with respect to (ω, Ω).*

Actually given any primitive homology class $\alpha \in \mathrm{H}_1(D, \mathbb{Z})$, the homology class $\tilde{\alpha} \in \mathrm{H}_2(X, \mathbb{Z})$ represented as a trivial S^1-bundle over a geodesic in D in the class α can be realized as the special Lagrangian torus fibre in Theorem 1.1. Due to the dimensional coincidence, one has $\mathrm{Sp}(1) = \mathrm{SU}(2)$ and thus X is hyperKähler. Let $\check{X}$ be the hyperkähler rotation with the Calabi-Yau metric and holomorphic volume form given by

$$\begin{aligned} \check{\Omega} &= \omega - \mathrm{i} \cdot \mathrm{Im}\, \Omega, \\ \check{\omega} &= \mathrm{Re}\, \Omega. \end{aligned} \tag{1.1}$$

Then the special Lagrangian fibration $X \to B$ becomes an elliptic fibration $\check{X} \to \mathbb{C}$ after hyperKähler rotation. Collins–Jacob–Lin further proved that

Theorem 1.2 (cf. [17]). *The fibration $\check{X} \to \mathbb{C}$ admits a compactification to a* rational elliptic surface *$\check{Y} \to \mathbf{P}^1$ by adding an I_d fibre over ∞, where $d = (-K_Y)^2$. In other words, we have the following commutative diagram.*

$$\begin{array}{ccccc} & \overset{\text{HK rotation}}{\curvearrowright} & & & \\ X & & \check{X} & \hookrightarrow & (\check{Y}, \mathrm{I}_d) \\ \downarrow & & \downarrow & & \downarrow \\ \mathbb{R}^2 & & \mathbb{C} & \longrightarrow & (\mathbf{P}^1, \infty) \end{array}$$

Note that $X = \check{X}$ as topological spaces. In particular, $\mathrm{H}_k(X; \mathbb{Z}) = \mathrm{H}_k(\check{X}; \mathbb{Z})$. We also remark that in the case of $Y = \mathbb{P}^2$, then $\check{X}$ is exactly the fibrewise compactification of the superpotential of $\mathbb{P}^2$ and a special case of Theorem 1.4 below.

The third author in [16] introduced the notion of large complex structure limits for pairs from the view point of the original SYZ conjecture. We say that (Y_t, D_t), $t \in (0, 1]$, a 1-parameter family of pairs of del Pezzo surfaces Y_t of degree d with a smooth anti-canonical divisor D_t is converging to a large complex structure limit if the limit $Y_t \to Y_0$ is a del Pezzo surface and $D_t \to D_0$ with D_0 being an irreducible nodal curve. We will denote $\alpha_t \in \mathrm{H}_1(D_t, \mathbb{Z})$ the vanishing cycle. Let $\pi_t : X_t = Y_t \backslash D_t \to B_t$ be the special Lagrangian fibration in Theorem 1.1 with fibre class $\tilde{\alpha}_t$.

Here we explain why this is a reasonable definition of large complex structure limit. Kontsevich–Soibelman [44] modified the original SYZ conjecture: the Calabi–Yau manifolds approaching to a large complex structure limit will Gromov–Hausdorff converge to an affine manifold with singularity. The conjecture is proved for the case of K3 surfaces [33, 54]

and compact hyperKähler manifolds with Lagrangian fibrations [32] and for Fermat type Calabi–Yau hypersurfaces [49][2]. Therefore, the collapsing of the SYZ fibration is usually viewed as the characterization of the large complex structure limit from the SYZ point of view. Now we compare the above SYZ collapsing picture with the semi-stable degenerations of K3 surfaces [46] studied by Kulikov. The semi-stable degenerations of K3 surfaces are classified into type I, II, III: the type I degenerations correspond to non-collapsing degenerations with the non-compact version studied in [50]. In the type II and type III degenerations, the metric K3 surfaces have collapsing limits and their Gromov–Hausdorff limits are harder to analyze. On one hand, the type II degeneration would lead to an interval as the Gromov–Hausdorff limits with respect to suitable scaling of the metrics [37, 39]. On the other hand, type III degenerations have their collapsing limits as an integral affine spheres with singularities and is the conjectural description of large complex structure limit [44, 54]. The key distinguishing feature of the latter two cases is that the collapsing limits have different dimensions. While the Tian–Yau spaces, are known as the bubbling limits of K3 surfaces, intuitively can be viewed as non-compact analogues of K3 surfaces. From the local model of the Tian–Yau spaces, one can see the geometry has a 2-dimensional collapsing limit near infinity when D_t degenerates [16]. Moreover, the third author and R. Takahashi recently proved that there is a global collapsing, i.e. with suitable scaling of the metrics, the Tian–Yau metrics Gromov–Hausdorff converge to a 2-dimensional affine manifold with singularities [51]. Therefore, the authors believe that the above definition of large complex structure limits of pairs is a reasonable one from the metric perspective.

With the above understanding and the motivation from the Gross–Siebert program, the authors earlier conjectured that

Conjecture 1. *The limiting complex affine manifold, i.e. the limit of complex affine structure on B_t coincides with the affine manifold with singularity in the work of Carl–Pumperla–Siebert* [9].

In the previous work, the authors proved

Theorem 1.3. [47] *Conjecture 1 holds in the case when $d = 9$.*

In this paper, we will extend the SYZ mirror symmetry of [16] to its compactification: providing the recipe for superpotentials of del Pezzo surfaces from the SYZ fibration constructed in [17].

Theorem 1.4 (=Theorem 3.1)**.** *Let (Y_t, D_t), $t \in [0, 1]$, be a 1-parameter family of pairs of del Pezzo surfaces Y_t and smooth anti-canonical divisors D_t. Assume that Y_0 is a smooth del Pezzo surface and D_0 is an irreducible nodal anti-canonical divisor of Y_0. Set $X_t = Y_t \setminus D_t$. Then the rational elliptic surfaces $\check{Y}_t$, $t \neq 0$ from Theorem 1.2 converge to the distinguished rational elliptic surface $\check{Y}_e$, which is the minimal smooth compactification of the Landau–Ginzburg mirror superpotential of the del Pezzo surfaces, viewed as monotone symplectic manifolds.*

[2]However, there are no results in the literature of comparison between the collapsing limits with the affine structures being used in the Gross–Siebert program to the authors knowledge. The result in [49] seems pretty close to such a statement but one requires stronger regularity on the solutions of real Monge–Ampère equations.

In particular, the limiting affine structure of the special Lagrangian fibration in the del Pezzo surfaces can be computed from $\check{Y}_e$. We further compute explicitly the limiting complex affine manifolds for the case del Pezzo surfaces of degree eight in Section 4.2 and for degree three and four in Section 5.

Remark 1.5. The slogan is "the mirror is given by the limit of the hyperKähler rotations towards the large complex structure limit." This seems to be a new phenomenon and doesn't appear in the K3 cases with respect to the mirror map in Gross–Wilson [34].

Remark 1.6. Ruddat and Siebert proved that Friedman's period points give monomial functions in the canonical coordinates of the base of the large complex structure limit degeneration [55], which may give another interpretation of Theorem 3.1. On the other hand, we point out that the limit of complex affine structures of the SYZ fibrations towards the large complex structure limit in the sense of [16] are different from the integral affine structure used in [9] except for the $\mathbf{P}^2$ case, which is a coincidence.

The above theorem provides an understanding of SYZ mirror symmetry from the perspective of the metrics and hyper-Kähler rotation. An interesting feature of the result is the following: the superpotentials (together with the correct complex structures) of the mirror involves the enumeration of holomorphic discs and thus depends on the global geometry of the del Pezzo surfaces. On the other hand, the Tian–Yau metric and the special Lagrangian fibration only depend on the non-compact part. This is a weak evidence that the Tian–Yau metric may detect some global geometry for some specific compactification. This kind of statement may help to understand the behavior of the Calabi-Yau metrics and the authors would pursue it in the future.

Now we explain why the limit $\check{Y}_e$ is indeed the correct mirror. Recall that from the Torelli theorem of the Looijenga pairs [30], there exists a distinguished complex structure $(\check{Y}_e, \check{D}_e)$ which has trivial periods in the deformation family of Looijenga pairs. Hacking–Keating [36] explains how to construct the mirror of a Lefschetz fibration $w\colon M \to \mathbb{C}$, where M is a Weinstein manifold. Furthermore, various versions of homological mirror symmetry are proved with A-side categories of M and B-side categories of $(\check{Y}_e, \check{D}_e)$. In the case we consider in this paper, $\check{Y}_e$ is a rational elliptic surface with $\check{D}_e$ being an I_d-fibre, then M can be realized as a complement of a smooth anti-canonical divisor in a del Pezzo surface. On the other hand, T. Collins, A. Jacob, and the third author constructed special Lagrangian fibrations on the complement of a smooth anti-canonical divisor in del Pezzo surfaces of degree d and on the complement of an I_d-fibre in rational elliptic surfaces. Moreover, the special Lagrangian fibrations on the two geometries are dual to each other with respect to a suitable mirror map when one chooses the exact Tian–Yau metric on the complement in the del Pezzo surface and the distinguished complex structure on the rational elliptic surface [16, 17]. This is mirror symmetry incorporating both A and B models on both geometries.

In the second part of this paper, we construct the mirrors for del Pezzo surfaces from the perspective in symplectic geometry, using the gluing scheme of [12, 40] based on immersed Lagrangian Floer theory [4, 23, 24, 57]. The immersed Lagrangians that we use are essentially the nodal singular fibers of the SYZ fibration (up to Lagrangian isotopy), which form the sources of quantum corrections and play a crucial role in (partial) compactification of the incomplete SYZ mirror constructed from merely smooth SYZ fibers.

In [12], Cho, Hong and the first author found a method of constructing mirrors by gluing deformation spaces of immersed SYZ Lagrangian fibers. A key ingredient is to establish and solve equations for Fukaya isomorphisms between the objects. The upshot is that there exists a canonical A_∞ functor from the Fukaya category to the matrix factorization category of the resulting LG model. The method was applied to construct the mirrors of punctured Riemann surfaces using Seidel's immersed Lagrangians. In [40], Hong, Kim and the first author studied the deformation and obstruction for nodal immersed spheres, and applied the method to construct the mirrors of two-plane Grassmannians.

In this paper, we consider del Pezzo surfaces of degree ≥ 3 which comes from smoothings of toric Gorenstein Fano surfaces. These are smoothings of A_n singularities, and we can construct a collection of immersed Lagrangians using A_n local models.

The case of $n = 0$ corresponds to $\mathbb{C}^2$, which has a special Lagrangian fibration with exactly one nodal singular fiber. The fibration can be understood as 'pushing in the corner' of the toric moment image of $\mathbb{C}^2$. Mirror construction using such a fibration for $\mathbb{C}^2$ were found by the celebrated work of Auroux [5] in the study of SYZ mirrors for various interesting examples of toric surfaces.

As in [12, 40], the mirror is constructed by gluing the unobstructed deformation spaces of these immersed Lagrangians, which will be denoted as $\mathbf{L}_{i,j}$ for certain indices i, j. Due to the nature of mirror construction from symplectic geometry, the result is a rigid analytic variety. What is important is that such a mirror is exactly the analytification of $\check{X}_e$. This is the reverse direction of mirror symmetry statement comparing to the work of Hacking–Keating [35]. More precisely, we prove the following theorem:

Theorem 1.7 (Theorem 6.19)**.** *Let X be a symplectic smoothing of a toric Gorenstein Fano surface with a monotone symplectic form, and let D be a smooth anti-canonical divisor. Let $\check{X}$ be the complex surface constructed as follows. First, we take the (multiple) blowing up of the toric variety $X_{\check{\Delta}}$ at every special point $z_i = -1$ in the i-th toric divisor for (n_i+1)-times (where $n_i + 1$ is the multiplicity of the i-th toric fixed point of X_Δ). We define $\check{X}$ to be the complement of the strict transform of all the toric divisors of $X_{\check{\Delta}}$. Then there is an A_∞ functor $\mathrm{Fuk}(X - D) \to D^b(\check{X} + \Lambda_+^2)$ that is injective on the morphism spaces of $\mathbf{L}_{i,j}$.*

Remark 1.8. The multiple blowing up of $X_{\check{\Delta}}$ above is a rational elliptic surface as in Theorem 1.2. Thus, we have shown that the Lagrangian Floer construction agrees with Theorem 3.1 for these cases.

The existence of the A_∞ functor and the injectivity on reference Lagrangians follow from the general theory in [12]. The main additional ingredient here is the local mirror construction for smoothings of A_n singularities (see Section 6.1) and blowing up over the Novikov ring.

The notations for the Novikov ring, its maximal ideal and the Novikov field are:

$$\Lambda_0 := \left\{ \sum_{i=0}^{\infty} a_i \mathbf{T}^{A_i} \mid a_i \in \mathbb{C}, A_i \geq 0 \text{ and increases to } +\infty \right\},$$
$$\Lambda_+ := \left\{ \sum_{i=0}^{\infty} a_i \mathbf{T}^{A_i} \mid a_i \in \mathbb{C}, A_i > 0 \text{ and increases to } +\infty \right\},$$
$$\Lambda := \left\{ \sum_{i=0}^{\infty} a_i \mathbf{T}^{A_i} \mid a_i \in \mathbb{C}, A_i \text{ increases to } +\infty \right\}.$$

The group of elements invertible in Λ_0 will also be important:

$$\Lambda_0^{\times} := \left\{ \sum_{i=0}^{\infty} a_i \mathbf{T}^{A_i} \in \Lambda_0 \mid A_0 = 0 \text{ and } a_0 \neq 0 \right\}.$$

A Lagrangian torus is equipped with flat $(\Lambda_0^{\times})^2$-connections; a Lagrangian nodal sphere is equipped with boundary deformations in $\{(u,v) \in \Lambda_0 : \mathrm{val}\,(uv) > 0\}$, where u and v are associated with the two immersed sectors at the nodal self-intersection. In general, the gluing of these charts results in a variety defined over Λ. On the other hand, when the immersed Lagrangians are constructed nicely so that they are in the same energy level, the gluing between them that solves the isomorphism equations does not involve the formal $\mathbf{T}$ parameter, and the resulting space is an Λ_0-extension of a variety over $\mathbb{C}$. This is why we have $\check{X} + \Lambda_+^2$ in the above theorem.

Acknowledgment. The authors would like to thank S.-T. Yau and B. Lian for their constant encouragement and support. They also thank CMSA at Harvard for providing a warm and comfortable working environment. The first author express his deep gratitude to Cheol-Hyun Cho, Hansol Hong and Yoosik Kim on several related collaborative works and a lot of motivating ideas. The third author would like to thank P. Hacking, Yuji Okada, and B. Siebert for the explanation on their related works. The third author also wants to thank T. Collins and A. Jacob for discussion on the earlier collaborations which motivated the project. The authors would all want to thank the anonymous reviewer for the precious comments and suggestions. The first author is supported by the Simons Collaboration Grant #580648. The second author is supported by the Simons Collaboration on HMS Grant. The third author is supported by the Simons Collaboration Grant # 635846 and NSF grant DMS #2204109.

2. Torelli theorem of log Calabi–Yau surfaces

In this section, we recall basic notions and properties of Looijenga pairs which will be used throughout this paper.

Definition 2.1 (cf. [30, 36])**.** A *Looijenga pair* $(\check{Y}, \check{D})$ is a pair consisting of a smooth projective surface $\check{Y}$ and a *singular* cycle $\check{D} \in |-K_{\check{Y}}|$. By adjunction, the arithmetic genus $p_a(\check{D}) = 1$, which implies that $\check{D}$ is either an irreducible nodal $\mathbf{P}^1$ or a cycle of smooth rational curves. A *log Calabi–Yau surface with maximal boundary* is a Looijenga pair $(\check{Y}, \check{D})$ where $\check{Y}$ is a smooth rational projective surface.

For a log Calabi–Yau pair $(\check{Y}, \check{D})$, it has been proven in [30, Lemma 1.3] that after blowing up some nodes in $\check{D}$, the resulting pair $(\check{Z}, \check{F})$, where $\check{F}$ is the reduced inverse image of $\check{D}$, admits a toric model $(\check{Y}_{\mathrm{tor}}, \check{D}_{\mathrm{tor}})$; namely, there is a birational morphism of pairs $(\check{Z}, \check{F}) \to (\check{Y}_{\mathrm{tor}}, \check{D}_{\mathrm{tor}})$ such that

- $\check{Y}_{\mathrm{tor}}$ is a smooth projective toric variety and $\check{D}_{\mathrm{tor}}$ is the toric boundary;
- the pair $(\check{Z}, \check{F})$ is obtained by successive blowups at interior points of the components of $\check{D}_{\mathrm{tor}}$, and $\check{F}$ is the strict transform of $\check{D}_{\mathrm{tor}}$.

Definition 2.2. The data $(\check{Y}, \check{D}) \leftarrow (\check{Z}, \check{F}) \to (\check{Y}_{\mathrm{tor}}, \check{D}_{\mathrm{tor}})$ is called *a toric model* of $(\check{Y}, \check{D})$.

2.1. **Torelli theorem for log CY surfaces with maximal boundary.** We begin by recalling a standard cohomology computation. Let $(\check{Y}, \check{D})$ be a log Calabi–Yau surface with maximal boundary. Put $\check{X} := \check{Y} \setminus \check{D}$. Consider the long exact sequence of the relative homology for $(\check{Y}, \check{X})$

$$0 \to \mathrm{H}_3(\check{Y}, \check{X}; \mathbb{Z}) \to \mathrm{H}_2(\check{X}; \mathbb{Z}) \to \mathrm{H}_2(\check{Y}; \mathbb{Z}) \to \mathrm{H}_2(\check{Y}, \check{X}; \mathbb{Z}) \to \mathrm{H}_1(\check{X}; \mathbb{Z}) \to 0. \tag{2.1}$$

Both sides in (2.1) are zero since $\mathrm{H}_1(\check{Y}; \mathbb{Z}) = \mathrm{H}_3(\check{Y}; \mathbb{Z}) = 0$. Via Lefschetz–Poincaré duality $\mathrm{H}_3(\check{Y}, \check{X}; \mathbb{Z}) \simeq \mathrm{H}^1(\check{D}; \mathbb{Z})$, we see that the sequence (2.1) is transformed into

$$0 \to \mathrm{H}^1(\check{D}; \mathbb{Z}) \to \mathrm{H}_2(\check{X}; \mathbb{Z}) \to \mathrm{H}_2(\check{Y}; \mathbb{Z}) \to \mathrm{H}^2(\check{D}; \mathbb{Z}) \to \mathrm{H}_1(\check{X}; \mathbb{Z}) \to 0. \tag{2.2}$$

Under the isomorphism $\mathrm{H}^2(\check{D}; \mathbb{Z}) \cong \mathbb{Z}^d$, the map $\mathrm{H}_2(\check{Y}; \mathbb{Z}) \to \mathrm{H}^2(\check{D}; \mathbb{Z})$ is identified with taking the signed intersection

$$\mathrm{H}_2(\check{Y}; \mathbb{Z}) \to \mathbb{Z}^d, \ [\gamma] \mapsto ([\gamma] \cdot [\check{D}_i])_{i=1}^d. \tag{2.3}$$

For each $1 \le i \le d$, let $[\check{D}_i]^\perp := \left\{ [\gamma] \in \mathrm{H}_2(\check{Y}; \mathbb{Z}) \;\middle|\; [\gamma] \cdot [\check{D}_i] = 0 \right\}$. Put $[\check{D}]^\perp := \cap_{i=1}^d [\check{D}_i]^\perp$. We then have a short exact sequence

$$0 \to \mathrm{H}^1(\check{D}; \mathbb{Z}) \to \mathrm{H}_2(\check{X}; \mathbb{Z}) \to [\check{D}]^\perp \to 0. \tag{2.4}$$

Since $(\check{Y}, \check{D})$ is log Calabi–Yau, there exists a unique (up to a constant) holomorphic two form $\check{\Omega}$ on $\check{X}$ with a simple pole along $\check{D}$. We then fix a basis $[\beta] \in \mathrm{H}_1(\check{D}; \mathbb{Z})$ by demanding

$$\int_\beta \mathrm{Res}\, \check{\Omega} = 1. \tag{2.5}$$

Following Friedman (see also the proof of Lemma 3.2), every cycle $[\gamma] \in [\check{D}]^\perp$ can be deformed into a cycle $[\tilde{\gamma}] \in \mathrm{H}_2(\check{X}; \mathbb{Z})$. Moreover, if $[\tilde{\gamma}']$ is an element in $\mathrm{H}_2(\check{X}; \mathbb{Z})$ whose image in $[\check{D}]^\perp$ is equal to $[\gamma]$, then

$$\int_{[\tilde{\gamma}']} \check{\Omega} - \int_{[\tilde{\gamma}]} \check{\Omega} \in \mathbb{Z}. \tag{2.6}$$

In particular, the map

$$\phi \colon [\check{D}]^\perp \to \mathbb{C}^*, \ [\gamma] \mapsto \exp\left(2\pi \mathrm{i} \cdot \int_{\tilde{\gamma}} \check{\Omega} \right) \tag{2.7}$$

is well-defined.

Definition 2.3. For a log Calabi–Yau surface with maximal boundary $(\check{Y}, \check{D})$, the map $\phi_{(\check{Y}, \check{D})} \in \mathrm{Hom}([\check{D}]^\perp, \mathbb{C}^*)$ obtained in (2.7) is called *the period point associated with* $(\check{Y}, \check{D})$.

The period map has another incarnation. For each line bundle L on $\check{Y}$ such that $L|_{\check{D}_i} \cong \mathcal{O}_{\check{D}_i}$, i.e. $L \in [\check{D}]^{\perp}$, its restriction to $\check{D}$ has $L_{\check{D}} \in \mathrm{Pic}^0(\check{D}) \cong \mathbb{C}^*$. Therefore, one naturally associate an element in $\mathrm{Hom}(\check{D}^{\perp}, \mathbb{C}^*)$ for each pair $(\check{Y}, \check{D})$. From the discussion in [21, p.21], the two notations of the periods actually coincide. Fix a deformation family of Looijenga pairs and a reference Looijenga pair $(\check{Y}_0, \check{D}_0)$. We identify $\mathrm{Hom}(\check{D}^{\perp}, \mathbb{C}^*) \cong \mathrm{Hom}(\check{D}_0^{\perp}, \mathbb{C}^*)$ via parallel transport for any Looijenga pair $(\check{Y}, \check{D})$ within the same deformation family. The weak Torelli theorem states that the periods classify the complex structure of the pairs within its deformation family.

Theorem 2.4 (Torelli theorem [30]). *The period $\phi_{(\check{Y},\check{D})} \in \mathrm{Hom}([\check{D}_0]^{\perp}, \mathbb{C}^*)$ determines the pair $(\check{Y}, \check{D})$ uniquely within its deformation type.*

From [21, Proposition 9.15 and Proposition 9.16], there are 10 deformation families of rational elliptic surfaces with I_d fibres, $d = 1, \ldots, 9$. More precisely, there is exactly one family for each $d \neq 8$ and two for $d = 8$. These correspond to 10 families of del Pezzo surfaces. Recall that the del Pezzo surfaces are either blowups of $\mathbf{P}^2$ at d points with $0 \leq d \leq 8$ in general position or $\mathbf{P}^1 \times \mathbf{P}^1$. We will explain which deformation families of rational elliptic surfaces with an I_8 fibre correspond to $\mathbb{F}_0 := \mathbf{P}^1 \times \mathbf{P}^1$ versus the Hirzebruch surface $\mathbb{F}_1$ later.

Within each deformation family, there is a distinguished rational elliptic surface whose period point is trivial by the Torelli theorem. The rational elliptic surface in each deformation with trivial periods can be characterized as follows. Let $(\check{Y}, \check{D})$ be a rational elliptic surface with trivial period point. Let $(\check{Y}, \check{D}) \leftarrow (\check{Z}, \check{F}) \rightarrow (\check{Y}_{\mathrm{tor}}, \check{D}_{\mathrm{tor}})$ be a toric model of $(\check{Y}, \check{D})$. Notice that $(\check{Z}, \check{F})$ and $(\check{Y}, \check{D})$ have the same period point under the identification $\mathrm{Hom}([\check{D}]^{\perp}, \mathbb{C}^*) \cong \mathrm{Hom}([\check{F}]^{\perp}, \mathbb{C}^*)$. Then $(\check{Y}, \check{D})$ has trivial period point if and only if $(\check{Z}, \check{F})$ does. Let $\check{D}_{\mathrm{tor},1}, \ldots, \check{D}_{\mathrm{tor},p}$ be the irreducible components of $\check{D}_{\mathrm{tor}}$. $(\check{Z}, \check{F})$ has trivial period point if and only if $(\check{Z}, \check{F})$ is obtained by blowing up the points $-1 \in \mathbb{C}^* = \check{D}_{\mathrm{tor},i} \setminus \bigcup_{j \neq i} \check{D}_{\mathrm{tor},j}$ in the toric coordinates on $(\check{Y}_{\mathrm{tor}}, \check{D}_{\mathrm{tor}})$ (cf. [30]).

This distinguished complex structure plays an essential role in the context of mirror symmetry. Hacking–Keating proved the homological mirror symmetry: let $\check{X} \to \mathbb{C}$ be the Landau-Ginzburg mirror of the Looijenga pair (Y, D). When $\check{X}$ is equipped with the exact symplectic form and (Y, D) has the distinguished complex structure, then the wrapped Fukaya category of $\check{X}$ is isomorphic to the derived category of coherent sheaves on X [36]. Collins–Jacob–Lin also proved SYZ mirror symmetry between del Pezzo surfaces and rational elliptic surfaces with such distinguished complex structures. Here in this paper, we will explain how such distinguished complex structures arise naturally from the large complex structure limit.

Recall that rational elliptic surface $\check{Y}$ is extremal if its Modell–Weil group is finite. All the extremal rational elliptic surfaces are classified (see [52, p.77]).

2.2. **Periods of certain toric surfaces.** In this subsection, we will compute the period point of certain log Calabi–Yau surfaces with maximal boundary $(\check{Z}, \check{F})$ which arise naturally from mirror symmetry. Let us fix the following notation.

- Let $N = \mathbb{Z}^2$ and $M = \mathrm{Hom}(N, \mathbb{Z})$ be the dual lattice. Let $N_{\mathbb{R}} = N \otimes \mathbb{R}$ and $M_{\mathbb{R}} = M \otimes \mathbb{R}$ be the scalar extension of N and M respectively.

- Let $\Delta \subset M_{\mathbb{R}}$ be a reflexive polytope. Denote by Σ_Δ the normal fan of Δ and by $\mathbf{P}_\Delta$ the toric variety associated with Σ_Δ. Let $\nabla = \Delta^\vee \subset N_{\mathbb{R}}$ be the dual polytope of Δ. Note that Σ_Δ is equivalent to the face fan of ∇.
- Let Δ_0 (resp. ∇_0) be the set of vertices of Δ (resp. ∇).

We will tacitly assume that $\mathbf{P}_\Delta$ is *smooth*; in other words, $\nabla_0 = \nabla \cap N \setminus \{\mathbf{0}\}$. Let t_1, t_2 be the coordinate on $(\mathbb{C}^*)^2$. Consider the superpotential

$$W\colon (\mathbb{C}^*)^2 \to \mathbb{C},\ (t_1,t_2) \mapsto \sum_{n\in\nabla_0} t^n.\ (\text{Here } t^n := t_1^{n_1}t_2^{n_2}.)$$

We may regard W as a *section* of the anti-canonical bundle on $\mathbf{P}_\nabla$, that is, we compactify the torus $(\mathbb{C}^*)^2$ into a projective toric surface $\mathbf{P}_\nabla$ in a way such that W extends to a section of the anti-canonical bundle on $\mathbf{P}_\nabla$. Let $\check{Y}_{\text{tor}} \to \mathbf{P}_\nabla$ be the maximal projective crepant partial desingularization. In the present case, the resolution is achieved by taking a sequence of weighted blow ups at codimension two strata (which are torus invariant points) and $\check{Y}_{\text{tor}}$ is a smooth semi-Fano toric surface.

Lemma 2.5. *$\{W = 0\}$ does not meet any torus fixed point on $\mathbf{P}_\nabla$.*

Proof. To simply the notation, put $\Sigma = \Sigma_\nabla$. Denote by $\Sigma(1)$ the set of 1-cones in Σ. For $\rho \in \Sigma(1)$, by abuse of notation, we also denote its primitive generator (in the lattice M) by the same symbol ρ. Consider the homogeneous coordinate ring $\mathbb{C}[w_\rho : \rho \in \Sigma(1)]$. Then every section $t^n \in \mathrm{H}^0(\mathbf{P}_\nabla, -K_{\mathbf{P}_\nabla})$ can be identified with a monomial via

$$t^n \mapsto \prod_{\rho\in\Sigma(1)} w_\rho^{\langle n,\rho\rangle+1}. \tag{2.8}$$

Put $p = |\Sigma(1)|$ and $U_\Sigma = \mathbb{C}^p \setminus Z(\Sigma)$. Since $\mathbf{P}_\nabla$ is simplicial, $U_\Sigma/G \cong \mathbf{P}_\nabla$ is a geometric quotient with $G = \mathrm{Hom}(\mathrm{Cl}(\mathbf{P}_\nabla), \mathbb{C}^*)$ (cf. [19, Chapter 5]). The symbol w_ρ can be thought of as a coordinate function on U_Σ and the monomial in the right hand side of (2.8) is a G-equivariant function with respect to a certain character of G. The toric divisor D_ρ is the image of $\{w_\rho = 0\}$ under the projection

$$\pi\colon U_\Sigma \to U_\Sigma/G.$$

Since $\mathbf{P}_\nabla$ is simplicial, each torus invariant point is an intersection of two toric divisors. $D_\rho \cap D_\mu \neq \emptyset$ if and only if ρ and μ span a 2-cone in Σ. Recall that

$$\nabla = \{n \in N_{\mathbb{R}} \mid \langle n,\rho\rangle \geq -1,\ \forall \rho \in \Sigma(1)\}.$$

It follows that $n \in \nabla_0$ if and only if there are exactly two 1-cones, say ρ and μ, such that $\langle n,\rho\rangle = \langle n,\mu\rangle = -1$ (since $\mathbf{P}_\nabla$ is Fano). Fix $n \in \nabla_0$ and pick ρ and μ as above. Now in the superpotential

$$W = \sum_{n\in\nabla_0\cap N} \prod_{\rho\in\Sigma(1)} w_{\rho'}^{\langle n,\rho'\rangle+1},$$

there exists a unique monomial which contains neither w_ρ nor w_μ. Consequently

$$W|_{w_\rho=w_\mu=0} = \prod_{\substack{\rho'\in\Sigma(1)\\ \rho'\notin\{\rho,\mu\}}} w_{\rho'}^{\langle n,\rho'\rangle+1}.$$

If there is a point $w \in \mathbb{C}^p$ such that $w_\kappa = w_\rho = w_\mu = 0$ with $\kappa \neq \rho$ and $\kappa \neq \mu$, then $\{\kappa, \rho, \mu\}$ contains a primitive collection of Σ which implies that $w \in Z(\Sigma)$. We thus conclude that $W(w) \neq 0$ for any $w \in \pi^{-1}(D_\rho \cap D_\mu)$. □

Let $\Sigma_\nabla(1) = \{\rho_1, \ldots, \rho_p\}$. Write $\rho_i = \begin{bmatrix} a_{1i} & a_{2i} \end{bmatrix}^\intercal$. The matrix

$$A = \begin{bmatrix} a_{11} & a_{12} & \cdots & a_{1p} \\ a_{21} & a_{22} & \cdots & a_{2p} \end{bmatrix}$$

gives rise to a map $A\colon \mathbb{Z}^p \to M,\ e_i \mapsto \rho_i$ whose cokernel is finite. The dual $A^\intercal\colon N \to \mathbb{Z}^p$ induces for each i an injection

$$\mathbb{C}[\rho_i^\perp \cap N] \to \mathbb{C}[e_i^\perp \cap \mathbb{Z}^p],\ s_i \mapsto \prod_{j=1}^p w_{\rho_j}^{\langle n_i, \rho_j \rangle}$$

where n_i is a primitive generator of $\rho_i^\perp \cap N \cong \mathbb{Z}$ and s_i is the corresponding coordinate function on $\mathbb{C}^* = \operatorname{Spec}(\mathbb{C}[\rho_i^\perp \cap N])$.

Fix i from now on. We will write a point in $\mathbb{C}^p$ as $(w_{\rho_i}, \mathbf{w})$, where $\mathbf{w}$ is a vector indexed by $\Sigma(1) \setminus \{\rho_i\}$. Let us compute the intersection $\{W = 0\} \cap D_{\rho_i}$. As in the proof of Lemma 2.5, we write

$$W = \sum_{n \in \nabla_0 \cap N} \prod_{j=1}^p w_{\rho_j}^{\langle n, \rho_j \rangle + 1} \tag{2.9}$$

and regard W as a function on U_Σ. Restricting W to $w_{\rho_i} = 0$, we see that only two terms in (2.9) survive: the monomials t^n with $\langle n, \rho_i \rangle = -1$. We denote them by t^{q_1} and t^{q_2}. Then $\{W = 0\} \cap D_{\rho_i}$ is equal to

$$\left\{ (0, \mathbf{w}) \in U_\Sigma \;\middle|\; \prod_{j=1}^p w_{\rho_j}^{\langle q_1, \rho_j \rangle + 1} + \prod_{j=1}^p w_{\rho_j}^{\langle q_2, \rho_j \rangle + 1} = 0 \right\} \Big/ G$$

By our assumption, the face fan of ∇ is smooth. It follows that $q_1 - q_2$ is a primitive generator of $\rho_i^\perp \cap N$ and therefore

$$\begin{aligned} & \prod_{j=1}^p w_{\rho_j}^{\langle q_1, \rho_j \rangle + 1} + \prod_{j=1}^p w_{\rho_j}^{\langle q_2, \rho_j \rangle + 1} = 0 \\ \Leftrightarrow\ & \prod_{j=1}^p w_{\rho_j}^{\langle q_1 - q_2, \rho_j \rangle} = -1 \\ \Leftrightarrow\ & s_i = -1. \end{aligned}$$

We summarize this into the following proposition.

Proposition 2.6. *Assume that $\mathbf{P}_\Delta$ is smooth. $\{W = 0\}$ and D_{ρ_i} can only meet at $-1 \in \mathbb{C}^* = \operatorname{Spec}(\mathbb{C}[\rho_i^\perp \cap N]) \subset D_{\rho_i}$.*

Let us focus on the MPCP desingularization now. Let $\check{D}_{\mathrm{tor}}$ be the union of toric divisors on $\check{Y}_{\mathrm{tor}}$. Since $\check{Y} \to \mathbf{P}_\nabla$ is crepant, W can be thought of as a section of $-K_{\check{Y}}$ as well. One immediately obtains the following corollary.

Corollary 2.7. *Assume that $\mathbf{P}_\Delta$ is smooth as before and regard W as a section of the anti-canonical bundle on $\check{Y}_{\mathrm{tor}}$. Let $(\check{Z}, \check{F})$ be the blow up of $(\check{Y}_{\mathrm{tor}}, \check{D}_{\mathrm{tor}})$ at $\{W = 0\} \cap \check{D}_{\mathrm{tor}}$ and let $\check{F}$ be the reduced inverse image of $\check{D}_{\mathrm{tor}}$. Then $(\check{Z}, \check{F})$ has trivial period point.*

Proof. Since $\{W = 0\}$ contains no torus fix points in $\mathbf{P}_\nabla$, the maximal projective crepant partial desingularization $\check{Y} \to \mathbf{P}_\nabla$ induces an isomorphism in a neighborhood of $\{W = 0\}$, because $\{W = 0\}$ only can intersect $\check{D}_{\mathrm{tor}}$ at interior points of each irreducible component of $\check{D}_{\mathrm{tor}}$. Combined with Proposition 2.6, we deduce that if they intersect, they must meet at $-1 \in \mathbb{C}^*$. Since $\check{Z}$ is obtained by a sequence of blow ups at those intersections, we conclude that $(\check{Z}, \check{F})$ must have trivial period point (cf. [30, Lemma 2.8 and Proposition 2.9]). □

3. From SYZ fibrations to LG superpotentials

In this section, we will prove the slogan "the limit of hyperKähler rotations towards the large complex structure limit gives the mirror." Recall that del Pezzo surfaces are either $\mathbf{P}^1 \times \mathbf{P}^1$ or blow up of $\mathbf{P}^2$ at d generic points, where $0 \leq d \leq 8$. Now given a holomorphic family of del Pezzo surfaces $p : \mathcal{Y} \to C$, there is a natural polarization $\mathcal{L}$ coming from the anti-canonical divisors. From the Riemann–Roch theorem, one gets that $h^0(Y, -K_Y)$ doesn't depend on the complex structure of the del Pezzo surface Y and $\mathrm{H}^i(Y, -K_Y)$ always vanishes. One deduces that $R^0 p_* \mathcal{L}$ is a vector bundle over C with fibre $\mathrm{H}^0(Y_c, -K_{Y_c})$ over c with $Y_c := p^{-1}(c)$. Then the total space of $R^0 p_* \mathcal{L}$ parametrizes the pairs of del pezzo surfaces with anti-canonical divisors. Outside a complex codimension one subset, a point in the total space of $R^0 p_* \mathcal{L}$ corresponds to a pair with smooth anti-canonical divisors. Now choosing a path $[0, 1]$ in the total space $R^0 p_* \mathcal{L}$ induces a 1-parameter family of pairs of del Pezzo surfaces Y_t of degree d with anti-canonical divisors D_t. Through out this section, we will assume that D_t are smooth for $t \neq 0$ and D_0 is irreducible and nodal[3].

Assume that D_t degenerates to an irreducible nodal curve D_0. Let $\alpha_t \in \mathrm{H}_1(D_t, \mathbb{Z})$ be the vanishing cycle. Let $\pi_t \colon X_t = Y_t \setminus D_t \to B_t$ be the special Lagrangian fibration produced in Theorem 1.2 with fibre class $\tilde{\alpha}_t$. Applying hyperkähler rotation to X_t yields another family $\check{X}_t \to \mathbb{C}$. By Theorem 1.2, we obtain a 1-parameter family of rational elliptic surfaces $\check{Y}_t$, $t \in (0, 1]$. This section is devoted to proving that

Theorem 3.1. *Assume that Y_0 is a generic del Pezzo surface. Then the rational elliptic surface $\check{Y}_t$ converges to the distinguished rational elliptic surface $\check{Y}_e$ in its deformation family, as $t \to 0$.*

From the Torelli theorem in the previous section, it suffices to prove that:

(∗) The period point $\phi_{\check{Y}_t}$ converges to the trivial homomorphism e as $t \to 0$.

In other words, the pair $(\check{Y}_t, \check{D}_t)$ converges to $(\check{Y}_e, \check{D}_e)$, the log Calabi–Yau surface with trivial period point.

Recall the following construction in [21, §3]

Lemma 3.2. *Let Y be a del Pezzo surface. Let $D \in |-K_Y|$ be an irreducible nodal curve or smooth curve. Then for each $\gamma \in [D]^\perp$, there exists a 2-cycle $\tilde{\gamma}$ of Y such that $[\tilde{\gamma}] = \gamma$ in Y and $\tilde{\gamma} \cap D = \emptyset$.*

[3]Notice that generic del Pezzo surfaces admits an irreducible nodal anti-canonical divisor.

Proof. One can write $\gamma = \sum_i a_i[C_i]$ with $a_i = \pm 1$ and C_i being smooth curves intersecting transversally at distinct points on D^{reg}. We can rearrange the signed intersections as $\sum(p_j - q_j)$. Let σ_j be a smooth curve in D^{reg} going from q_j to p_j and $\tau(\sigma_j)$ be a tube over σ_j in Y. We can glue $\tau(\sigma_j)$ with $\gamma \setminus \{p_j, q_j\}$ inductively and obtain $\tilde{\gamma}$. □

One can find a 1-parameter family of diffeomorphisms $f_t\colon Y_0 \cong Y_t$ with $t \in [0,1]$. Fix a neighborhood $N \subseteq Y_0$ of D_0. There exists an $\epsilon > 0$ such that $D_t \subseteq f_t(N)$ for $t < \epsilon$. Let $\{\gamma_1, \dots, \gamma_s\}$ be a basis of $[D_0]^\perp \subset \mathrm{H}_2(Y;\mathbb{Z})$ and $\{\tilde{\gamma}_1, \dots, \tilde{\gamma}_s\}$ be the corresponding deformed cycles in $X_0 := Y_0 \setminus D_0$. We can also regard $\tilde{\gamma}_i$ as a cycle in X_t. By shrinking the neighborhood N if necessary, we may assume that $f_t(\tilde{\gamma}_i) \cap D_t = \emptyset$ for $t < \epsilon$.

Lemma 3.3. *Let D_t be the degeneration as above and $X_t := Y_t \setminus D_t$. Let $\alpha_t \in \mathrm{H}_1(D_t;\mathbb{Z})$ be the homology class of the vanishing cycle. Let $\beta_t \in \mathrm{H}_1(D_t;\mathbb{Z})$ such that $\{\alpha_t, \beta_t\}$ is a symplectic basis of $\mathrm{H}_1(D_t;\mathbb{Z})$. Then $\{[\tilde{\alpha}_t], [\tilde{\beta}_t], [f_t(\tilde{\gamma}_1)], \dots, [f_t(\tilde{\gamma}_s)]\}$ is a basis of $\mathrm{H}_2(X_t;\mathbb{Q})$ for all $t \in [0,\epsilon]$.*

Proof. Adapting the discussion in §2.1 to (Y_t, D_t), we obtain an exact sequence

$$0 \to \mathrm{H}^1(D_t;\mathbb{Z}) \to \mathrm{H}_2(X_t;\mathbb{Z}) \to [D_t]^\perp \to 0. \tag{3.1}$$

Notice that $[D_t] = [D_0]$ in $\mathrm{H}^2(Y_t;\mathbb{Z})$. The result follows immediately. □

We will now study the period point associated with $(\check{Y}_t, D_t)$ as t approaches zero. From the setup of (Y_t, D_t), there is a smooth family of holomorphic 2-forms Ω_t on X_t for $t \in [0,1]$. Notice that $f_t^*\Omega_t|_{Y_0 \setminus N}$ converges to Ω_0. In particular, this implies that the period integrals $\int_{f_t^*(\tilde{\gamma}_i)} \Omega_t$ to $\int_{f_t^*(\tilde{\gamma}_i)} \Omega_0$ as $t \to 0$. In particular, $\int_{f_t^*(\tilde{\gamma}_t)} \Omega_t$ is bounded. Recall that

$$\check{\Omega}_t = \omega_t - \mathrm{i} \cdot \operatorname{Im} \Omega_t.$$

The exactness of the Tian–Yau metric ω_t implies that

$$\int_\delta \check{\Omega}_t = \int_\delta \omega_t - \mathrm{i} \cdot \int_\delta \operatorname{Im} \Omega_t = -\mathrm{i} \cdot \operatorname{Im} \int_\delta \Omega_t \tag{3.2}$$

for all $\delta \in \mathrm{H}_2(X_t;\mathbb{Z})$. Hence it suffices to compute the integrals

$$\int_\delta \Omega_t, \ \delta \in \mathrm{H}_2(X_t;\mathbb{Z}),$$

on the Tian–Yau space.

Lemma 3.4. *Let $\mu_t := \operatorname{Res}_{D_t} \Omega_t$. We have*

(1) $\dfrac{\mathrm{i}}{2} \displaystyle\int_{D_t} \mu_t \wedge \bar{\mu}_t \to \infty$ *as* $t \to 0$*;*

(2) $\displaystyle\int_{\alpha_t} \mu_t$ *is bounded.*

Proof. Let $p \in D_0^{\mathrm{sing}}$. Choose a coordinate chart V of Y around p such that the degeneration $D_t \to D_0$ is given by $xy = t$ in $\mathbb{C}^2$. Set $E_t = \{xy = t + O(t)\}$. For $t \neq 0$, we may write

$$\frac{\mathrm{d}x \wedge \mathrm{d}y}{xy - t} = \frac{\mathrm{d}(xy - t)}{xy - t} \wedge \eta_t.$$

We see that

$$\mathrm{Res}_{E_t}\left(\frac{\mathrm{d}x\wedge\mathrm{d}y}{xy-t}\right)=\eta_t|_{E_t}=-\left.\frac{\mathrm{d}x}{x}\right|_{E_t}+O(t)=\left.\frac{\mathrm{d}y}{y}\right|_{E_t}+O(t).$$

Let $\epsilon>0$ be small and set

$$E_{t,\epsilon}:=\{(x,y)\mid |x|^2+|y|^2<\epsilon\}\cap E_t.$$

Since $\lim_{t\to 0}\Omega_t=\Omega_0$ exists, there is a holomorphic function $f(x,y)$ with $f(0,0)\neq 0$ such that

$$\Omega_t|_V=\frac{f(x,y)\mathrm{d}x\wedge\mathrm{d}y}{xy-t}+O(t).$$

It follows that

$$\begin{aligned}\frac{\mathrm{i}}{2}\int_{D_t}\mu_t\wedge\bar{\mu}_t&\geq\frac{\mathrm{i}}{2}\int_{E_{t,\epsilon}}\mu_t\wedge\bar{\mu}_t+O(t)\\&\geq\frac{\mathrm{i}}{2}\int_{E_{t,\epsilon}}|f(x,y)|^2\frac{\mathrm{d}x\wedge\mathrm{d}\bar{x}}{|x|^2}+O(t)\\&\geq C\int_0^{2\pi}\int_{r=t/\sqrt{\epsilon}}^{\sqrt{\epsilon}}\frac{\mathrm{d}r\mathrm{d}\theta}{r}+O(t)\to\infty\end{aligned}$$

as $t\to 0$. This proves the item (1).

Now we prove the item (2). For $\epsilon>0$, we fix a point $(x_0,y_0)\in E_{t,\epsilon}$. Then

$$r_t(\theta):=(x_0e^{\mathrm{i}\theta},y_0e^{-\mathrm{i}\theta}),\ \theta\in[0,2\pi),$$

is a closed curve in $E_{t,\epsilon}$ representing α_t. We can compute

$$\int_{\alpha_t}\mu_t=\int_0^{2\pi}f(r_t(\theta))\mathrm{d}\theta$$

and conclude that it is bounded for $\epsilon\ll 1$ since f is continuous at $(0,0)$. □

Now we are ready to prove Theorem 3.1.

Proof of Theorem 3.1. One first observe that

$$\int_{\tilde{\beta}_t}\Omega_t=2\pi\int_{\beta_t}\mu_t\to\infty,$$

where the first equality comes from residue calculation and Lemma 3.4 implies the asymptotics. Normalize Ω_t to $\tilde{\Omega}:=(\int_{\tilde{\beta}_t}\Omega_t)^{-1}\Omega_t$ for $t\neq 0$ and rescale the Tian–Yau metric accordingly, which does not change the complex structure of the hyperKähler rotation $\check{X}_t$ and thus does not change $\check{Y}_t$. Notice that $\tilde{\beta}_t$ is the generator of the image of $\mathrm{H}^1(\check{D}_t,\mathbb{Z})$ in (2.2), and thus the normalization here is exactly the one in (2.5). Therefore, all the periods of $\check{Y}_t$ converge to zero as $t\to 0$ under the normalization. In fact, note that the cycle $f_t(\tilde{\gamma}_i)$ is only defined up to an element in $\mathrm{Im}(\mathrm{H}^1(D_t,\mathbb{C})\to\mathrm{H}_2(X_t,\mathbb{C}))=\mathrm{Span}_{\mathbb{C}}\{\tilde{\alpha}_t,\tilde{\beta}_t\}$. Under the normalization, we see that

$$\exp\left(2\pi\mathrm{i}\cdot\int_{f_t(\tilde{\gamma}_i)}\tilde{\Omega}_t\right)\to 1\text{ as }t\to 0$$

due to the fact that

$$\int_{f_t(\tilde{\alpha})} \Omega_t \Big/ \int_{f_t(\tilde{\beta})} \Omega_t \to 0, \text{ as } t \to 0.$$

We conclude by Lemma 3.4 and the observation above that all periods converge to zero under the normalization. This also implies that $\check{Y}_t$ converges to the unique rational elliptic surface $\check{Y}_e$ with trivial periods from Theorem 2.4. □

The following is proved in Appendix A

Theorem 3.5. *Consider a del Pezzo surface of degree d as a monotone symplectic manifold and let $W\colon (\mathbb{C}^*)^2 \to \mathbb{C}$ be the mirror Landau–Ginzburg superpotential. Then it can be compactified to a rational elliptic surface $\check{Y}$ with an I_d-fibre and with trivial periods. In particular, $\check{Y}$ is extremal when $d = 9, 8, 6, 3, 2, 1$ with singular configuration* $\mathrm{I}_9\mathrm{I}_1^3, \mathrm{I}_8\mathrm{I}_2\mathrm{I}_1^2, \mathrm{I}_6\mathrm{I}_3\mathrm{I}_2\mathrm{I}_1, \mathrm{I}_3\mathrm{IV}^*\mathrm{I}_1, \mathrm{I}_2\mathrm{III}^*\mathrm{I}_1, \mathrm{I}_1\mathrm{II}^*\mathrm{I}_1$.

4. Limiting Complex affine structure of special Lagrangian fibration in $\mathbf{P}^1 \times \mathbf{P}^1$

We first review the definition of complex affine structures [38]. With the notation in Section 1, recall that $X \subseteq Y$ is a Calabi–Yau surface with a holomorphic volume form Ω and let $\pi_\alpha\colon X \to B$ be a special Lagrangian fibration constructed in [17] with a choice of $\alpha \in H_1(D, \mathbb{Z})$. Denote by B_0 the complement of the discriminant locus. Fix a reference point $u_0 \in B_0$ and $\gamma \in \mathrm{H}_1(L_{u_0}, \mathbb{Z})$. Let $u \in B_0$ and $\phi\colon [0,1] \to B_0$ be a path with $\phi(0) = u_0$ and $\phi(1) = u$. Denote by $C_{\gamma,\phi}$ the $(n-1)$-cycle fibration over $\phi([0,1])$ such that fibre over $\phi(t)$ is the 1-cycle in $L_{\phi(t)}$ which is the parallel transport of γ along ϕ. We define

$$x_\gamma(u) := \int_{C_\gamma} \operatorname{Im} \Omega.$$

If $\{\gamma_i\}$ is a basis of $\mathrm{H}_1(L_{u_0}, \mathbb{Z})$, then $x_{\gamma_i}(u)$, $i = 1, 2$, form a coordinate system near the reference point u_0. It is straightforward to check that the transition functions fall in $\mathrm{GL}(2, \mathbb{Z}) \ltimes \mathbb{R}^2$, and thus they define an integral affine structure on B_0. It is worth noticing that given an affine line (with rational slope) passing through $u \in B_0$, its tangent vector determines a cycle $\gamma \in \mathrm{H}_1(L_u, \mathbb{R})$ (or $\mathrm{H}_1(L_u, \mathbb{Z})$) and vice versa. Therefore, we will denote such an affine line by $l_{u,\gamma}$ or simply by l_γ if no confusion occurs.

Remark 4.1. If one chooses a sequence of points $u_i \to u_*$ from a sector, where u_* falls in the discriminant locus, then $\lim_{i\to\infty} x_{\gamma_i}(u_i)$ exists. Therefore, one may take u_* as the reference point as well.

Remark 4.2. The germ of affine structures on a punctured disc is determined by the affine monodromy around the puncture. In particular, if the affine structure comes from a special Lagrangian fibration as above, the germ only depends on the monodromy of the fibration.

For the case $Y = \mathbf{P}^2$, the suitable hyperKähler rotation $\check{X}$ of X can always be compactified to an extremal rational elliptic surface [16]. In particular, the base B with the complex affine structure of the special Lagrangian fibration π_α as an affine manifold with singularities is independent of the choice of $\alpha \in \mathrm{H}_1(D, \mathbb{Z})$. Actually, this is true in a more general setting.

Proposition 4.3. *Fix a pair (Y, D) and $\alpha, \alpha' \in \mathrm{H}_1(D, \mathbb{Z})$. The bases B, B' of the special Lagrangian fibrations $\pi_\alpha, \pi_{\alpha'}$ with their complex affine coordinates are isomorphic as affine manifolds with singularities.*

Proof. It suffices to prove that there exists a diffeomorphism $\psi\colon X \to X$ such that $\pi_\alpha = \pi_{\alpha'} \circ \psi$. Then the induced map of ψ gives a diffeomorphism $B \cong B'$ identifying the complex affine structures. In particular, this answers a question of Hacking–Keating [35, §7.4].

For any $\alpha, \alpha' \in \mathrm{H}_1(D, \mathbb{Z})$, there exists 1-parameter family of pairs $(Y_t, D_t), t \in [0, 1]$ such that $(Y_0, D_0) = (Y_1, D_1) = (Y, D)$ and the parallel transport sends α' to α. Such a 1-parameter family induces a diffeomorphism ϕ of (X, ω_{TY}) for the exact Tian-Yau metric ω_{TY}, sending the $[\tilde{\alpha}]$ to $[\tilde{\alpha}']$. Let Ω (and Ω') be the meromorphic 2-form on Y with simple pole along D and $\int_{[\tilde{\alpha}]} \Omega \in \mathbb{R}_+$ (and $\int_{[\tilde{\alpha}']} \Omega' \in \mathbb{R}_+$ respectively). Then $\phi^*\Omega$ is a closed 2-form with vanishing self-wedge and thus defines an integrable complex structure. Moreover, the same underlying space $\underline{X}$ as X with Kähler form $\phi^*\omega_{TY}$ and holomorphic volume form $\phi^*\Omega$ is an ALH* gravitational instanton since the volume growth is still $r^{\frac{4}{3}}$. Now we have two ALH* gravitational instantons $(\underline{X}, \omega_{TY}, \Omega)$ and $(\underline{X}, \omega_{TY}, \phi^*\Omega)$ as well as a morphism $\phi\colon X \to X$ satisfying $\phi^*[\omega_{TY}] = [\omega_{TY}]$ and $\phi^*[\Omega] = [\Omega']$. From the Torelli theorem of the ALH^* gravitational instantons [18, Theorem 3.9], there exists a diffeomorphism $\phi' : X \to X$ such that $\phi'^*\phi^*\omega_{TY} = \omega_{TY}$ and $\phi'^*\phi^*\Omega = \Omega'$. Taking $\psi = \phi \circ \phi'$, then $\psi_*[\tilde{\alpha}] = [\tilde{\alpha}']$. Any special Lagrangian torus of class $[\tilde{\alpha}]$ (and $[\tilde{\alpha}']$) must be a fibre of the special Lagrangian fibration with fibre class $[\tilde{\alpha}]$ (and $[\tilde{\alpha}']$ respectively). Thus, ψ sends the special Lagrangian fibration in X with fibre class $[\tilde{\alpha}]$ to the special Lagrangian fibration in X with fibre class $[\tilde{\alpha}']$ as claimed.

□

4.1. **The integral affine structure from Carl–Pumperla–Siebert.** Let Y be a del Pezzo surface and D be a smooth anti-canonical divisor. Carl–Pumperla–Siebert [9] construct the mirror for the pair (Y, D). We now describe the integral affine manifold with singularities, denoted as B_{CPS}, used in their construction when $Y = \mathbf{P}^1 \times \mathbf{P}^1$.

We first start with $\mathbb{R}^2$ with the standard integral affine structure. There are four singularities located at $(\pm 1/2, \pm 1/2)$ with the monodromy around each of the singularities conjugate to $\begin{pmatrix} 1 & 1 \\ 0 & 1 \end{pmatrix}$.

To cooperate with the standard affine structure on $\mathbb{R}^2$, the branch cuts for the singularities are put at the following locations:

$$
\begin{aligned}
l_1^+ &= \left\{ \left(\frac{1}{2} + t, \frac{1}{2} \right) \,\middle|\, t \geq 0 \right\}, & l_1^- &= \left\{ \left(\frac{1}{2}, \frac{1}{2} + t \right) \,\middle|\, t \geq 0 \right\}, \\
l_2^+ &= \left\{ \left(-\frac{1}{2}, \frac{1}{2} + t \right) \,\middle|\, t \geq 0 \right\}, & l_2^- &= \left\{ \left(-\frac{1}{2} + t, \frac{1}{2} \right) \,\middle|\, t \leq 0 \right\}, \\
l_3^+ &= \left\{ \left(-\frac{1}{2} + t, -\frac{1}{2} \right) \,\middle|\, t \leq 0 \right\}, & l_3^- &= \left\{ \left(-\frac{1}{2}, -\frac{1}{2} + t \right) \,\middle|\, t \leq 0 \right\}, \\
l_4^+ &= \left\{ \left(\frac{1}{2}, -\frac{1}{2} + t \right) \,\middle|\, t \leq 0 \right\}, & l_4^- &= \left\{ \left(\frac{1}{2} + t, -\frac{1}{2} \right) \,\middle|\, t \geq 0 \right\}.
\end{aligned}
$$

B_{CPS} is constructed by discarding the sectors bounded by $l_i^{\pm}$ in $\mathbb{R}$ and gluing the branch cuts $l_i^{\pm}$ with the affine transformations shown in Figure 1. However, this will not be

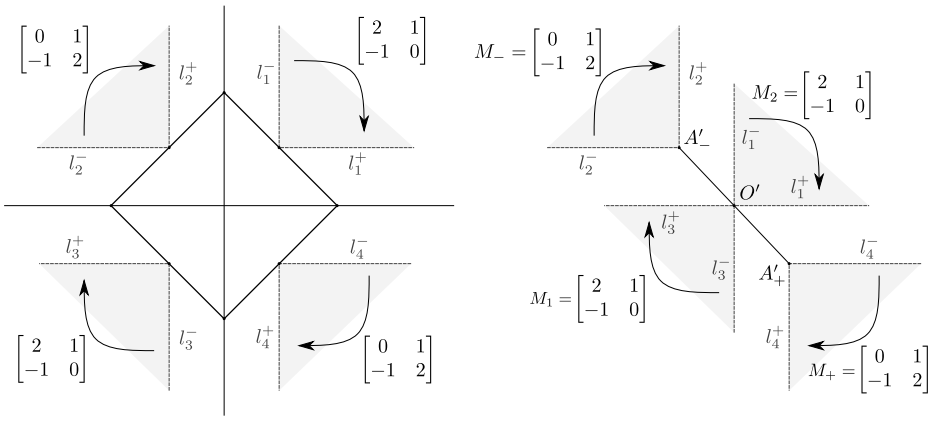

FIGURE 1. The affine structure on B_{CPS} and its limit B'_{CPS}.

the limit of the base of the special Lagrangians constructed in [17]. We will compare the latter to a degeneration of B_{CPS}, denoted by B'_{CPS}. Roughly speaking, B'_{CPS} is the integral affine manifold obtained by collapsing two of the singularities together. Let $A'_-(-1/2, 1/2), O' = (0,0), A'_+ = (1/2, -1/2)$ be the three singularities. We will choose the branch cuts as

$$\begin{aligned} l_1^+ &= \left\{(t,0) \,\middle|\, t \geq 0\right\}, & l_1^- &= \left\{(0,t) \,\middle|\, t \geq 0\right\}, \\ l_2^+ &= \left\{\left(-\frac{1}{2}, \frac{1}{2}+t\right) \,\middle|\, t \geq 0\right\}, & l_2^- &= \left\{\left(-\frac{1}{2}+t, \frac{1}{2}\right) \,\middle|\, t \leq 0\right\}, \\ l_3^+ &= \left\{(t,0) \,\middle|\, t \leq 0\right\}, & l_3^- &= \left\{(0,t) \,\middle|\, t \leq 0\right\}, \\ l_4^+ &= \left\{\left(\frac{1}{2}, -\frac{1}{2}+t\right) \,\middle|\, t \leq 0\right\}, & l_4^- &= \left\{\left(\frac{1}{2}+t, -\frac{1}{2}\right) \,\middle|\, t \geq 0\right\}. \end{aligned}$$

Then B'_{CPS} is defined similarly as the complement of the sectors bounded by $l_i^{\pm}$ in $\mathbb{R}^2$ with the standard integral affine structure, where we glue the branch cuts $l_i^{\pm}$ with respect to the affine structures as in Figure 1. Notice that it is not clear that B_{CPS} and B'_{CPS} are related by moving worms introduced in [45].

4.2. **Explicit calculation of the complex affine structure.** In this section, we will compute the limit of the complex affine structure of the special Lagrangian fibration of $X_t = \mathbf{P}^1 \times \mathbf{P}^1 \setminus D_t$, where D_t are smooth anti-canonical divisors degenerating to a nodal curve D_0.

Lemma 4.4. *Assume that σ is a fibrewise involution on X. Then σ induces an involution $\underline{\sigma}$ on B. If furthermore $\sigma^*(\operatorname{Im}\Omega) = -\operatorname{Im}\Omega$, then the fixed locus $Fix(\underline{\sigma}) \subseteq B$ defines an affine line with a rational slope.*

Proof. The first part of the lemma is straightforward. Notice that $\mathrm{Fix}(\underline{\sigma})$ is a manifold. Let $p \in \mathrm{Fix}(\underline{\sigma})$ and take p as the reference point of the local affine coordinate chart. Let l_γ be the affine line tangent to $p \in \mathrm{Fix}(\underline{\sigma})$ with $\gamma \in \mathrm{H}_1(L_p, \mathbb{R})$. Then one has $l_{\sigma_*(\gamma)} = \underline{\sigma}(l_\gamma) = l_\gamma$. In particular, $l_\gamma \subseteq \mathrm{Fix}(\underline{\sigma})$, and thus the fixed locus of $\underline{\sigma}$ is simply the affine line l_γ. It is worth noticing that the induced action of σ on $\mathrm{H}_1(L_u, \mathbb{R})$ is defined over $\mathbb{Z}$. In particular, if $n = 2$ and $\sigma \neq \mathrm{id}$, then l_γ has a rational slope. □

The hyperKähler rotation $\check{X}_t$ can be compactified into a rational elliptic surface $\check{Y}_t$ and $\lim_{t\to 0} \check{Y}_t =: \check{Y}$ converges in the moduli. Together with the hyperKähler rotation relation (1.1) and the fact that the Tian–Yau metric is exact, it is sufficient to compute the affine structure induced by $\mathrm{Im}\,\check{\Omega}$.

For the case $Y = \mathbf{P}^1 \times \mathbf{P}^1$ and D_t a family of smooth elliptic curves degenerating to a nodal curve D_0, as we have explained, $\check{Y} = \lim_{t\to 0} \check{Y}_t$ is the extremal rational elliptic surface with singular configuration $I_8 I_2 I_1^2$ with $\check{D}$ being the I_8 fibre at infinity. The toric model $(\check{Y}_{\mathrm{tor}}, \check{D}_{\mathrm{tor}})$ of $(\check{Y}, \check{D})$ is given by the maximal projective crepant partial desingularization $\check{Y}_{\mathrm{tor}} \to \mathbf{P}_\nabla$, where

$$\nabla = \mathrm{Conv}\{(1,0),(0,1),(-1,0),(0,-1)\}.$$

The superpotential in this case is

$$W\colon (\mathbb{C}^*)^2 \to \mathbb{C},\ (t_1,t_2) \mapsto t_1 + t_2 + \frac{1}{t_1} + \frac{1}{t_2}. \tag{4.1}$$

Regarding W as an element in $\mathrm{H}^0(\check{Y}_{\mathrm{tor}}, -K_{\check{Y}_{\mathrm{tor}}}) = \mathrm{H}^0(\mathbf{P}_\nabla, -K_{\mathbf{P}_\nabla})$, we see that $\check{Y} = \check{Z}$ is obtained by blowing up at $\{W = 0\} \cap \check{D}_{\mathrm{tor}}$.

The critical values of the superpotential W are $0, \pm 4 \in B := \mathbb{C}$, which will be denoted by $O, A_\pm$ respectively in the sequel. Note that the fibre over O is an I_2 fibre, while the fibres over $A_\pm$ are I_1 fibres. Let $\check{\Omega}$ be the unique (up to a constant) meromorphic $(2,0)$-form on $\check{Y}$ with a simple pole along $\check{D}$ such that the complex conjugation on $\check{Y}$ is a fibre-preserving involution and thus the fixed locus of the induced action on B is an affine line. Explicitly, $\check{\Omega}$ is the pullback of a meromorphic top form under $\check{Y} \to \check{Y}_{\mathrm{tor}}$ which comes from a sequence of blowups at smooth points in $\check{D}_{\mathrm{tor}}$. In what follows, we will compute integrations of $\check{\Omega}$ over certain Lefschetz thimbles which are not contained in the exceptional locus of $\check{Y} \to \check{Y}_{\mathrm{tor}}$. We thus can compute these integrals on the maximal torus $(\mathbb{C}^*)^2$. In the sequel, we shall omit the pullback and simply write

$$\check{\Omega} = \mathrm{i} \cdot \frac{\mathrm{d}t_1}{t_1} \wedge \frac{\mathrm{d}t_2}{t_2} \tag{4.2}$$

if no confusion occurs. Here (t_1, t_2) stands for the coordinates on $(\mathbb{C}^*)^2 \subset \check{Y}_{\mathrm{tor}}$.

Denote by q the coordinate on B. Look at the diagram

$$\begin{array}{ccc} (t_1,t_2) & (\mathbb{C}^*)^2 & \xrightarrow{W} \mathbb{C}. \\ \big\downarrow & \big\downarrow{\scriptstyle \mathrm{pr}_2} & \\ t_2 & \mathbb{C}^* & \end{array} \tag{4.3}$$

For general $q \in \mathbb{C}$, the pre-image $W^{-1}(q)$ is an elliptic curve with four points removed.

Lemma 4.5. *The ramification points t_2 of the double cover $W^{-1}(q) \to \mathbb{C}^*$ induced from the vertical arrow in (4.3) satisfy $(t_2^2 + 1 - qt_2)^2 - 4t_2^2 = 0$.*

Proof. Compute

$$t_1 + t_2 + \frac{1}{t_1} + \frac{1}{t_2} - q = 0 \;\Leftrightarrow\; t_1^2 t_2 + t_1 t_2^2 + t_2 + t_1 - q t_1 t_2 = 0$$
$$\Leftrightarrow\; t_2 t_1^2 + (t_2^2 + 1 - q t_2) t_1 + t_2 = 0.$$

We see that t_2 is a ramification point if and only if $(t_2^2 + 1 - qt_2)^2 - 4t_2^2 = 0$. □

Making use of (4.1), we can write (4.2) as

$$\mathrm{i} \cdot \frac{\mathrm{d}q \wedge \mathrm{d}t_2}{2t_1 t_2 + t_2^2 + 1 - q t_2} \tag{4.4}$$

whenever $t_1^2 \neq 1$. Moreover, from $W(t_1, t_2) - q = 0$, we can solve

$$t_1 = f_\pm(t_2) := \frac{-(t_2^2 + 1 - qt_2) \pm \sqrt{(t_2^2 + 1 - qt_2)^2 - 4t_2^2}}{2t_2}. \tag{4.5}$$

Here we have chosen the branch cut to be the non-positive real axis to define the square root. For a nonzero complex number $z \notin \mathbb{R}_-$, we define

$$\sqrt{z} := \exp\left(\frac{1}{2}\log z\right),$$

where

$$\log z = \log|z| + \mathrm{i}\theta,\ \theta \in (-\pi, \pi).$$

Substituting t_1, we may rewrite (4.4) and get

$$\check{\Omega} = \mathrm{i} \cdot \frac{\mathrm{d}q \wedge \mathrm{d}t_2}{\pm\sqrt{(t_2^2 + 1 - qt_2)^2 - 4t_2^2}} \tag{4.6}$$

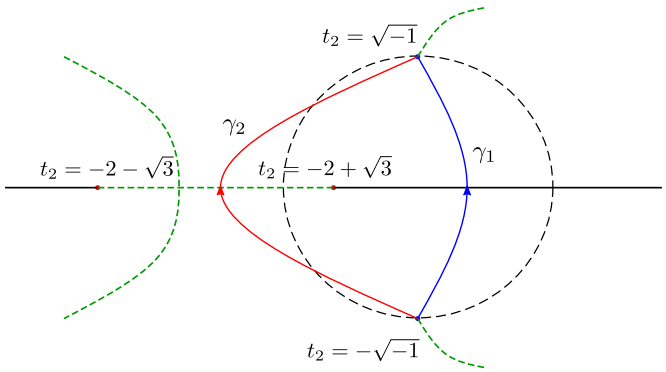

FIGURE 2. The t_2-plane at $q = -2$. There are four ramification points: $t_2 = \pm\,\mathrm{i}$ and $t_2 = -2 \pm \sqrt{3}$. The green dashed line segments indicate the branch cuts we chose, i.e., the loci where $(t_2^2 + 1 - qt_2)^2 - 4t_2^2 \leq 0$.

Each line segment of $\{q \in \mathbb{R}\}$ between $O, A_\pm$ is an affine line. Notice that due to the monodromy the corresponding 1-cycles in the fibres for each of the affine line segments $\overline{\infty A_-}, \overline{A_- O}, \overline{O A_+}, \overline{A_+ \infty}$ are not the same after parallel transport.

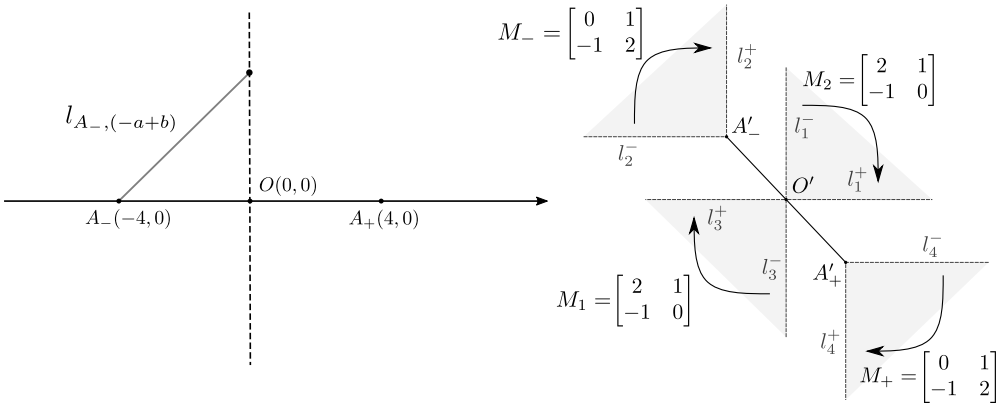

FIGURE 3. Base of the SYZ fibration in coordinate q and B'_{CPS}.

For the rest of this section, we will take O as the reference point of the affine structure (see Remark 4.1). We will restrict ourselves to the region $\operatorname{Im} q \geq 0$. Let $a(q), b(q)$ be the vanishing thimbles from O, A_- up to parallel transport via a path contained in the region $\operatorname{Im}(q) > 0$ into a fibre over q with the orientation such that

(1) $\int_{a(q)} \operatorname{Re} \check{\Omega} < 0$, if $q \in \overline{A_- O}$ and
(2) $\int_{b(q)} \operatorname{Re} \check{\Omega} > 0$, if $\operatorname{Im}(q) > 0$ near A_-.

Let us describe the cycles $a(q)$ and $b(q)$ explicitly. Let $\gamma_i \colon [0,1] \to \mathbb{C}^*$ be a parametrization of the oriented smooth curve drawn in FIGURE 2. The cycle ∂a can be parameterized by

$$\gamma_{\partial a}(s) = \begin{cases} (\gamma_1(2s), f_+(\gamma_1(2s))), & 0 \leq s \leq 1/2, \\ (\gamma_1(2-2s), f_-(\gamma_1(2-2s)), & 1/2 \leq s \leq 1, \end{cases} \tag{4.7}$$

where $f_\pm(t)$ is defined in (4.5). We equip ∂a with the orientation induced from this parametrization to achieve the item (1) above.

Lemma 4.6. *Under the parametrization (4.7), the item (1) above holds; namely*

$$\int_{a(q)} \operatorname{Re} \check{\Omega} < 0, \text{ for } q \in \overline{A_- O}.$$

Proof. Note that

$$\int_{a(q)} \check{\Omega} = -\int_{a(q)} \iota_{\partial/\partial q} \check{\Omega} \wedge \mathrm{d}q = -\int_0^q \int_{\partial a(q)} (\iota_{\partial/\partial q} \check{\Omega}) \mathrm{d}q.$$

Since $q < 0$, the result will follow if we can show that

$$\operatorname{Re}\left(\int_{\partial a(q)} \iota_{\partial/\partial q} \check{\Omega} \right) < 0.$$

Deforming the curve, we may assume $\gamma_1(\theta) = \exp(\mathrm{i}\theta)$, $\theta \in [-\theta_0, \theta_0] \subseteq [-\pi, \pi]$, with the counterclockwise orientation. By (4.6),

$$\int_{\partial a(q)} \iota_{\partial/\partial q} \check{\Omega} = 2 \int_{-\theta_0}^{\theta_0} \frac{-\exp(\mathrm{i}\theta)\mathrm{d}\theta}{\sqrt{\exp(2\mathrm{i}\theta)((2\cos\theta - q)^2 - 4)}}.$$

Note that $(2\cos\theta - q)^2 - 4 > 0$ for all $\theta \in (-\theta_0, \theta_0)$. We deduce that

$$\sqrt{\exp(2\mathrm{i}\theta)((2\cos\theta - q)^2 - 4)} = \exp(\mathrm{i}\theta)\sqrt{(2\cos\theta - q)^2 - 4}$$

and therefore

$$\int_{-\theta_0}^{\theta_0} \frac{-\exp(\mathrm{i}\theta)\mathrm{d}\theta}{\sqrt{\exp(2\mathrm{i}\theta)((2\cos\theta - q)^2 - 4)}} = \int_{-\theta_0}^{\theta_0} \frac{-\mathrm{d}\theta}{\sqrt{(2\cos\theta - q)^2 - 4}} < 0.$$

□

Likewise, we can equip ∂b with an orientation through γ_2 to achieve item (2). Starting from $t_2 = -\mathrm{i}$, we parameterize ∂b via

$$\gamma_{\partial b}(s) = (\gamma_2(s), f_+(\gamma_2(s))),\ 0 \le s \ll 1.$$

Let $\{\gamma_2(s_i) \mid 0 < s_1 < \cdots < s_k < 1\}$ be the intersection of γ_2 and the branch cut. When γ_2 meets the branch cut, the curve $\gamma_{\partial b}$ enters a different sheet and we shall exchange $f_\pm(t)$. In other words, ∂b can be parameterized by

$$\gamma_{\partial b}(s) = \begin{cases} (\gamma_2(2s), f_+(\gamma_2(2s)), & 0 \le s \le s_1/2 \\ (\gamma_2(2s), f_-(\gamma_2(2s)), & s_1/2 \le s \le s_2/2 \\ \quad\vdots & \quad\vdots \\ (\gamma_2(2s), f_\pm(\gamma_2(2s)), & s_k/2 \le s \le 1/2, \\ (\gamma_2(2-2s), f_\mp(\gamma_2(2-2s)), & 1/2 \le s \le 1 - s_k/2, \\ \quad\vdots & \quad\vdots \\ (\gamma_2(2-2s), f_+(\gamma_2(2-2s)), & 1 - s_2/2 \le s \le 1 - s_1/2, \\ (\gamma_2(2-2s), f_-(\gamma_2(2-2s)), & 1 - s_1/2 \le s \le 1. \end{cases}$$

and we equip ∂b with the induced orientation of this parametrization. Here the sign depends on the parity of k. For instance, if $k = 1$, then we shall pick f_- for $s_1/2 \le s \le 1/2$ and f_+ for $1/2 \le s \le 1 - s_1/2$. Similar to the proof of Lemma 4.6, we can prove the follow lemma, which shows that the orientation fulfills the requirement.

Lemma 4.7. *For $q \in \overline{A_- O}$, we have*

$$\int_{b(q)} \mathrm{Re}\,\check{\Omega} = 0 \text{ and } \int_{b(q)} \mathrm{Im}\,\check{\Omega} < 0.$$

Lemma 4.8. *If the reference point is changed to a point near O, then $\langle \partial a, \partial b \rangle = -2$, where $\langle , \rangle$ is the natural pairing of the fibre torus.*

Proof. Since the intersection number is topological, we can compute $\langle \partial a, \partial b \rangle$ at q_0 near A_-. It is clear that $\langle \partial a, \partial b \rangle = \pm 2$. To pin down the sign, we notice that if $\ell_{\partial a}$ (resp. $\ell_{\partial b}$) denotes the curve starting from q_0 with the direction such that

$$\int_{\partial a} \check{\Omega} \in \mathbb{R} \ \left(\text{resp. } \int_{\partial b} \check{\Omega} \in \mathbb{R}\right)$$

and increases, then we have

$$\langle v_{\partial a}, v_{\partial b} \rangle > 0 \tag{4.8}$$

with respect to the orientation on the base $\mathbb{C}$, where $v_{\partial a}$ (resp. $v_{\partial b}$) is the tangent vector of $\ell_{\partial a}$ (resp. $\ell_{\partial b}$) at q_0 pointing in the direction in which the symplectic area is increasing. Since $\langle \partial a, \partial b \rangle$ and $\langle v_{\partial a}, v_{\partial b} \rangle$ differ by a sign, this completes the proof. □

Now define another set of affine coordinates by $x := x_{\partial(a-b)}$ and $y := x_{\partial(a+b)}$.

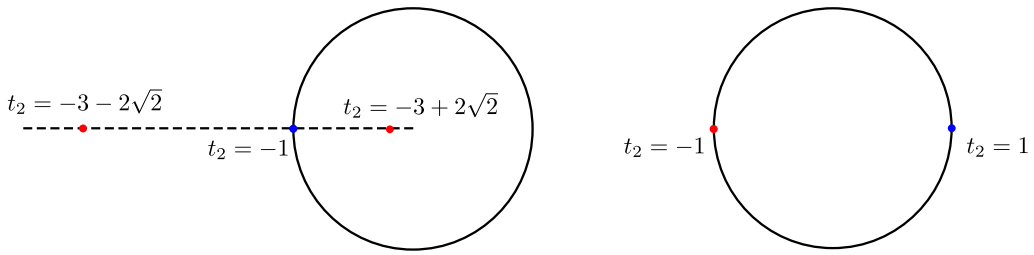

(a) $q = -4$ (b) $q = 0$

FIGURE 4. When q moves from -4 to 0 in $\mathbb{R}$, two of the ramifications (red marks in figure (a)) collapse to $t_2 = -1$ in figure (b) along the real axis $t_2 \in \mathbb{R}$. Note that $t_2 = -1$ in figure (a) is a double ramification. One can also check that the ramifications marked in blue travel along the semicircles $t_2 = (2 + q \pm \sqrt{q^2 + 4q})/2$ when q moves from -4 to 0.

Lemma 4.9. *The affine line* $\operatorname{Im} q = 0$ *between* O *and* A_- *satisfies* $x + y = 0$. *The same is true for the affine line* $\operatorname{Im} q = 0$ *between* O *and* A_+.

Proof. We will prove the former statement. The proof of the latter statement is similar. It suffices to prove that $x_{\partial a} = 0$; in other words, we have to show that

$$\int_{a(q)} \check{\Omega} \in \mathbb{R} \tag{4.9}$$

where $a(q)$ is the vanishing thimble from O to $q \in \overline{OA_-}$. From the proof of Lemma 4.6, one can directly see that (4.9) holds. However, we shall give a more conceptual proof which will be useful later.

We can choose a such that the image of ∂a (over $q \in \overline{OA_-}$) under the projection pr_2 in diagram (4.3) is given by a path γ connecting two ramification points $(2 + q \pm \sqrt{q^2 + 4q})/2$ and passing through the positive real axis $\{t_2 \in \mathbb{R}_+\}$. We may also assume that γ is invariant under complex conjugation as well (cf. FIGURE 5). Now we have

$$\int_{\partial a} \iota_{\partial/\partial q} \check{\Omega} = 2 \int_\gamma \mathrm{i} \cdot \frac{\mathrm{d}t_2}{\sqrt{(t_2^2 + 1 - qt_2)^2 - 4t_2^2}}. \tag{4.10}$$

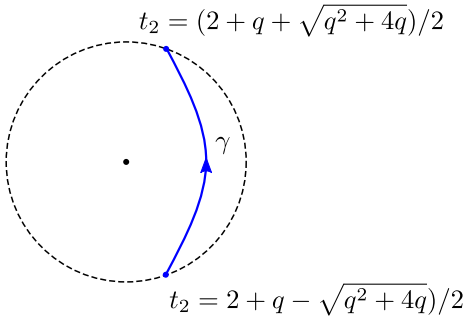

FIGURE 5. The image of $\partial a(q)$ under the projection pr_2.

Let $\gamma_+ := \gamma \cap \{\mathrm{Im}\, t_2 \geq 0\}$ and $\gamma_- := \gamma \cap \{\mathrm{Im}\, t_2 \leq 0\}$. Notice that $\bar{\gamma}_+ = -\gamma_-$ (orientation reversing). We can write

$$\begin{aligned}
&\int_\gamma \frac{\mathrm{d}t_2}{\sqrt{(t_2^2 + 1 - qt_2)^2 - 4t_2^2}} \\
&\quad = \int_{\gamma_+} \frac{\mathrm{d}t_2}{\sqrt{(t_2^2 + 1 - qt_2)^2 - 4t_2^2}} + \int_{\gamma_-} \frac{\mathrm{d}t_2}{\sqrt{(t_2^2 + 1 - qt_2)^2 - 4t_2^2}} \\
&\quad = \int_{\gamma_+} \frac{\mathrm{d}t_2}{\sqrt{(t_2^2 + 1 - qt_2)^2 - 4t_2^2}} - \int_{\gamma_+} \frac{\mathrm{d}\bar{t}_2}{\sqrt{(\bar{t}_2^2 + 1 - q\bar{t}_2)^2 - 4\bar{t}_2^2}} \in \mathrm{i} \cdot \mathbb{R}.
\end{aligned}$$

It follows from (4.10) that

$$\int_{\partial a} \iota_{\partial/\partial q} \check{\Omega} \in \mathbb{R}$$

which implies

$$\int_{a(q)} \check{\Omega} = -\int_0^q \int_{\partial a} (\iota_{\partial/\partial q} \check{\Omega}) \mathrm{d}q \in \mathbb{R}$$

as desired. □

Let us examine the branch cut when $q = \mathrm{i}\xi \in \mathrm{i} \cdot \mathbb{R}_+$. We observe that the set $\{t_2 \in \mathbb{C}^* \mid (t_2^2 + 1 - \mathrm{i}\xi t_2)^2 - 4t_2^2 \leq 0\}$ is invariant under $t_2 \mapsto -\bar{t}_2$. Moreover, $\{t_2 \in \mathbb{C}^* \mid (t_2^2 + 1 - \mathrm{i}\xi t_2)^2 - 4t_2^2 \leq 0\} \cap \mathrm{i} \cdot \mathbb{R}_+ = \emptyset$. Indeed, if $t_2 = \mathrm{i}x$ with $x \in \mathbb{R}_+$,

$$(t_2^2 + 1 - \mathrm{i}\xi t_2)^2 - 4t_2^2 = (-x^2 + 1 + \xi x)^2 + 4x^2 > 0.$$

The following lemma shows that $\mathrm{i} \cdot \mathbb{R}_+$ is an affine ray.

Lemma 4.10. *Recall that the reference point is the origin O. We have*

$$x_{\partial(-a+b)}(q) = 0 \text{ for } q \in \mathrm{i} \cdot \mathbb{R}_+.$$

Proof. Denote by γ_1 and γ_2 the image of ∂a and ∂b under the projection pr_2 in (4.3). For $q = \mathrm{i} \cdot \xi \in \mathrm{i} \cdot \mathbb{R}_+$, we may assume the γ_i are smooth curves connecting two out of four ramifications that collapse to one point when $q \to 0$ (cf. FIGURE 6). By our choice of orientations, we see that the image of $\gamma_2 - \gamma_1$ is a closed curve on $\mathbb{C}^*$. As in the proof of

Lemma 4.9, we shall compute an integral of a holomorphic function over $\gamma_2 - \gamma_1$. We can deform γ_2 a bit and assume that $\gamma_2 - \gamma_1$ is symmetric with respect to the imaginary axis.

Write $\gamma_2 - \gamma_1 = \gamma_+ \cup \gamma_-$ where

$$\gamma_+ := \{p \in \gamma_2 - \gamma_1 \mid \operatorname{Re} p \geq 0\} \text{ and } \gamma_- := \{p \in \gamma_2 - \gamma_1 \mid \operatorname{Re} p \leq 0\}.$$

We see that γ_- and $-\bar{\gamma}_+$ are set-theoretically symmetric with respect to the imaginary axis, but the orientation is reversed.

The integrand is given by

$$\iota_{\mathrm{i}\partial/\partial\xi}\check{\Omega} = \pm\frac{\mathrm{d}t_2}{\sqrt{(t_2^2+1-qt_2)^2-4t_2^2}} =: F(t_2)$$

with $q \in \mathrm{i}\cdot\mathbb{R}_+$. Since the branch cut does not intersect $\mathrm{i}\cdot\mathbb{R}_+$, the integrand $F(t_2)$ satisfies $F(-\bar{t}_2) = -F(\bar{t}_2)$. Now for such a function $F(t_2)$,

$$\int_{\gamma_+} F(t_2) + \int_{\gamma_-} F(t_2) = \int_{\gamma_+} F(t_2) + \int_{\gamma_+} F(\bar{t}_2) \in \mathbb{R}$$

which implies the result. □

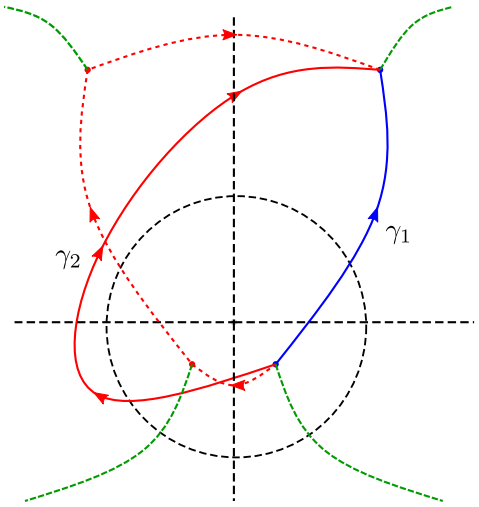

FIGURE 6

Next we will choose the branch cut of $A_\pm$ to be the affine line segments $\overline{\infty A_\pm}$ contained in $\{\mathrm{Im}(q) = 0\}$ as in FIGURE 3. If we move q across $\overline{\infty A_-}$ from $\mathrm{Im}(q) > 0$ to $\mathrm{Im}(q) < 0$, then the counter-clockwise monodromy around $A_\pm$ is given by

$$\partial a \mapsto \partial a + 2\partial b$$
$$\partial b \mapsto \partial b.$$

Therefore, the corresponding clockwise affine transformation is $M_\pm$ (cf. FIGURE 3).

Lemma 4.11. $x_{\partial(-a+b)}(q) - x_{\partial(-a+b)}(A_-) = 0$ *for* $q < -4$.

Proof. The argument used in Lemma 4.10 applies to this case. Denote again by γ_1 and γ_2 the image of ∂a and ∂b on the t_2-plane under the projection pr_2 in (4.3). For $q < -4$, we may assume the γ_i are smooth curves connecting two out of four ramifications that collapse to one point when $q \to -4$ (cf. FIGURE 7). We can deform γ_1 a bit and assume that $\gamma_2 - \gamma_1$ is symmetric with respect to the real axis.

Write $\gamma_2 - \gamma_1 = \gamma_+ \cup \gamma_-$ where

$$\gamma_+ := \{p \in \gamma_2 - \gamma_1 \mid \operatorname{Im} p \geq 0\}, \text{ and}$$
$$\gamma_- := \{p \in \gamma_2 - \gamma_1 \mid \operatorname{Im} p \leq 0\}.$$

We see that in the present case γ_- and $\bar{\gamma}_+$ are set-theoretically symmetric with respect to the real axis, but the orientation is reversed.

Since $\gamma_2 - \gamma_1$ does not intersect the branch cut on the real axis, it follows that the integrand $F(t_2)$ obeys the rule $F(\bar{t}_2) = -\bar{F}(t_2)$, and we have

$$\int_{\gamma_+} F(t_2) + \int_{\gamma_-} F(t_2) = \int_{\gamma_+} F(t_2) + \int_{\gamma_+} \bar{F}(t_2) \in \mathbb{R}.$$

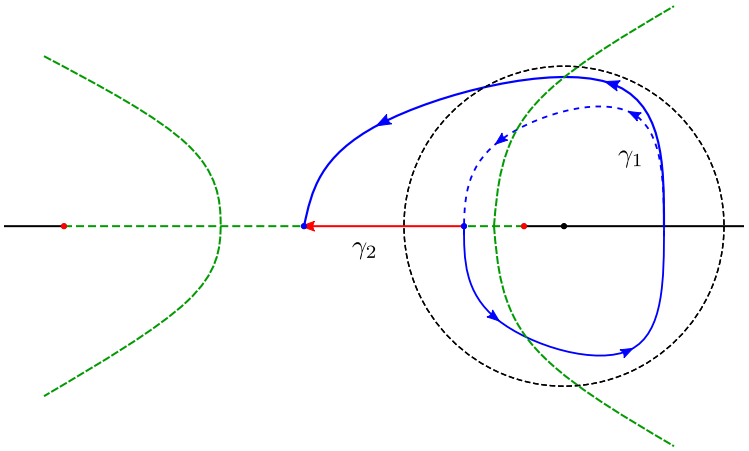

FIGURE 7. γ_1 (the blue solid curve) is the image of ∂a, and γ_2 (the red solid curve) is the image of ∂b. We can deform the upper part of γ_1 into the union of the blue dashed curve and γ_2.

□

The proof of the following lemma is deferred to Appendix B.

Lemma 4.12. *The affine line $l_{A_-,\partial b}$ intersects $l_{O,\partial(-a+b)}$.*

Now we will choose $\overline{\infty A_\pm}$, which is an affine ray by Lemma 4.11, to be the branch cuts from $A_\pm$. The monodromy $M_\pm$ coincides with the gluing transformation of cuts around $A'_\pm$ in B'_{CPS}. Thus, there exists an affine isomorphism Ψ between a punctured neighborhood of $A_\pm$ in B and a punctured neighborhood of $A'_\pm \in B'_{CPS}$ by Remark 4.2. With the scaling of the affine coordinates chosen appropriately, the affine isomorphism Ψ can be chosen such that

it can be extended to a neighborhood of $\overline{OA_-}$ in B. Moreover, by Lemma 4.9, the extended isomorphism will identify a neighborhood of $\overline{OA_-}$ in B with a that of $\overline{O'A'_-}$ in B'_{CPS} with $\Psi(\overline{OA_-}) = \overline{O'A'_-}$. Let M_1, M_2 be as in FIGURE 3. Then $M = M_1M_2$ is the monodromy around O. We will choose two branch cuts from O to be $\mathrm{i}\mathbb{R}_\pm$ with the gluing transformation M_1, M_2. From Lemma 4.10 and Remark 4.2, we can again extend the affine isomorphism Ψ to an affine isomorphism identifying a neighborhood of O with a neighborhood of O' such that $\Psi(\mathrm{i}\mathbb{R}_+)$ is the branch cut from O' in FIGURE 3.

Next let us denote the intersection of the affine lines $l_{A_-,\partial b}$ and $l_{O,\partial(-a+b)}$ by C. Then $C' = \Psi(C) = (0,1)$. Moreover, Ψ extends to an affine isomorphism from the triangle $OA_-C \subseteq B$ to $O'A_-C' \subseteq B_{CPS}$ by Lemma 4.9, Lemma 4.10, and Lemma 4.12. Again Lemma 4.10, Lemma 4.11, and Lemma 4.12 imply that such an affine isomorphism can be extended from the unbounded region in B surrounded by $l_{A_-,\partial(-a+b)}, l_{O,-\partial a}, l_{O,\partial(-a+b)}$ to the corresponding unbounded region in B_{CPS} as shown in FIGURE 3. By the symmetry $q \to \bar{q}$ and $q \to -\bar{q}$, the affine isomorphism extends to $\Psi\colon B \cong B'_{CPS}$.

Remark 4.13. Although the integral affine structures with singularities on B and B_{CPS} are different (even up to moving worms), the authors expect that the corresponding tropical counting of the $\mathbb{A}^1$-curves and the product structures of the algebra generated by theta functions are the same. The authors will leave it for future work.

Remark 4.14. It is worth noticing that the Mordell–Weil group of $\check{Y}_e$ is $\mathbb{Z}_4$ [53] (see also [56, p.102]) and thus gives a $\mathbb{Z}_4$-action on $\check{Y}_e$ which descends to the identity on the base of the elliptic fibration.

5. Limiting Complex Affine Structure for del Pezzo Surface of Degree 3 and 4

In this section, we will describe the limiting complex affine structure for del Pezzo surface of degree 3 and 4.

We first deal the the case of del Pezzo surface of degree 3 and recall the geometric setup: let $Y = \mathbb{P}^2$, D is a smooth cubic surface and X be the complement $X = Y \setminus D$. Then X admits a special Lagrangian fibration with respect to ω_{TY}, Ω from Theorem 1.1 and a suitable hyperKähler rotation $\check{X}$ with hyperKähler triple $(\check{\omega}, \check{\Omega})$ can be compactified to a rational elliptic surface $\check{Y}_9$ with an I_9-fibre from Theorem 1.2. It is known that there exists a unique rational elliptic surface with an I_9-fibre with singular configuration $I_9I_1^3$. The authors then use the geometry of $\check{Y}_9$ to computed the complex affine structure of the special Lagrangian fibration on X. It is given by the affine subspace of $\mathbb{R}^2$ as shown in Figure 8 and then glue the corresponding edges with the prescribed linear transformations. It is proved that there exists an $\mathbb{Z}_3 \oplus \mathbb{Z}_3$-action on $\check{X}$ preserving $(\check{\omega}, \check{\Omega})$ in [16, Corollary 5.11] and the proof therein. Denote t_1, t_2 be the local complex coordinates of $\check{Y}_9$, where t_1 is the fibre coordinate and t_2 is the base coordinate on $\mathbb{P}^1$. The first copy of $\mathbb{Z}_3$ is the Mordell-Weil group of $\check{Y}_9$ and acts as translation by holomorphic sections. In other words, it is of the form

$$t_1 \mapsto t_1 + \sigma(t_2), t_2 \mapsto t_2,$$

where σ is the holomorphic section. The second copy of $\mathbb{Z}_3$ preserves a holomorphic section of $\check{Y}_9$ and sends fibres to fibres. Thus, the second $\mathbb{Z}_3$-action descends to the base $\mathbb{P}^1$ of $\check{Y}_9$

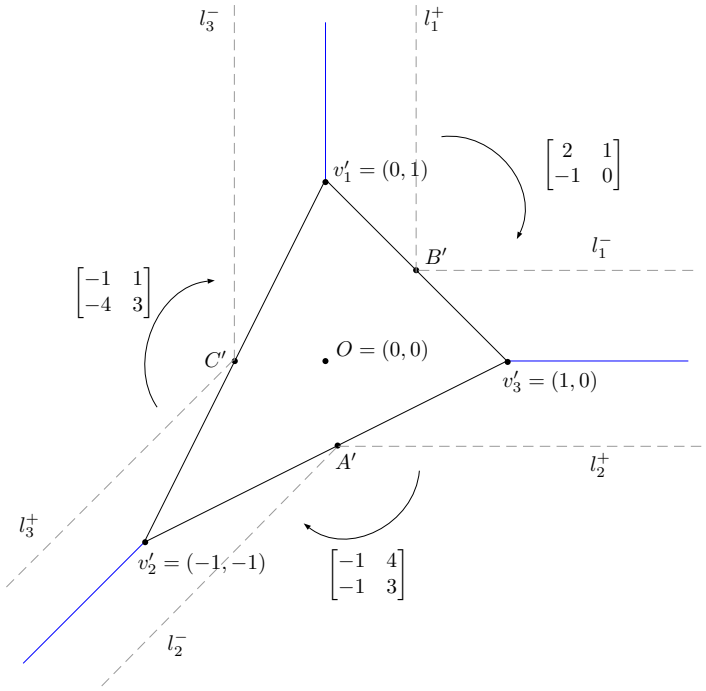

FIGURE 8. The limiting complex affine structure of special Lagrangian fibration in $\mathbf{P}^2$

and acts simply as the rotation

$$t_1 \mapsto t_1, t_2 \mapsto e^{2\pi i/3} t_2.$$

In particular, the fibres over $t_2 = 0, \infty$ are fixed. Let $r = (1,1) \in \mathbb{Z}_3 \oplus \mathbb{Z}_3$ and denote $\langle r \rangle \cong \mathbb{Z}_3$ be the subgroup generated by r. Since both $\mathbb{Z}_3$-action is fibration preserving, $\check{Y}_9/\langle r \rangle$ still admits an elliptic fibration structure. The I_9-fibre of $\check{Y}_9$ reduces to an I_3-fibre after the quotient. The three I_1-fibres are identified to a single I_1-fibre. The fibre over $t_2 = 0$ is set-wisely fixed by the action of $\langle r \rangle$ and after the quotient becomes an orbifold $\mathbb{P}^1$ with three orbifold singularities locally modeled by $\mathbb{C}^2/\mathbb{Z}_3$. Thus, the minimal resolution $\check{Y}$ of $\check{Y}_9/\langle r \rangle$ is a crepant resolution. From the formula of anti-canonical divisor for ramified cover, for instance [7, Lemma I.17.1], we have $\check{Y}$ is a again a rational elliptic surface and its singular configuration is $IV^* I_3 I_1$. We then have the following observations:

- consider the del Pezzo surface of degree 3 as a monotone symplectic manifold, then its mirror Landau-Ginzburg potential can be compactified to $\check{Y}$ from Theorem 3.5.
- The $\langle r \rangle$-action preserves $(\check{\omega}, \check{\Omega})$ on $\check{X}$ implies that the $\langle r \rangle$-action preserves (ω, Ω) on X and descends to a $\mathbb{Z}_3$-action on the complex affine structure of X. Therefore, the underlying space of $\check{X} \setminus \{t_2 = 0\}$, viewed as a subspace of X, admits a special Lagrangian fibration with respect to (ω, Ω). Moreover, the complex affine structure of this special Lagrangian fibration is the $\mathbb{Z}_3$-quotient of the complex affine structure of the special Lagrangian fibration in X.

- Recall that the complex affine structure of the the limiting special Lagrangian fibration of del Pezzo surfaces of degree 3 is determined by $\check{Y}$ by Theorem 3.1. Since $\check{Y} \to \check{Y}_9/\langle r \rangle$ is a crepant resolution, the complex affine structure from the limiting special Lagrangian fibration in del Pezzo surface of degree 3 is exactly the same as that of the special Lagrangian fibration in $\check{X} \setminus \{t_2 = 0\}$.

Now the $\mathbb{Z}_3$-action on the complex affine structure of the special Lagrangian fibration in $\mathbb{P}^2$ can be described as the linear transformation $\begin{pmatrix} 0 & 1 \\ -1 & -1 \end{pmatrix}$ restricting to the affine subspace in Figure 8. It is straight-forward to check that the transformation preserves the gluings listed Figure 8. Altogether, we reach the following conclusion:

Theorem 5.1. *The limiting complex affine structure for del Pezzo surface of degree* 3 *is a* $\mathbb{Z}_3$ *quotient of the complex affine structure of the special Lagrangian in* $\mathbb{P}^2$*. The* $\mathbb{Z}_3$*-action is generated by* $\begin{pmatrix} 0 & -1 \\ 1 & -1 \end{pmatrix}$*. Explicitly, it is given by the shaded affine subset of* $\mathbb{R}^2$ *in Figure 9 below with* $\overline{OB'}$ *identified with* $\overline{OC'}$ *and two vertical boundaries identified.*

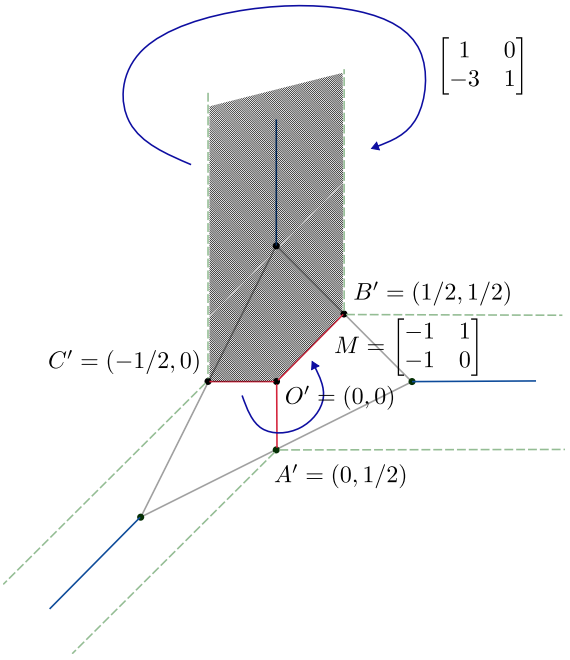

FIGURE 9. The limiting affine structure for del Pezzo surfaces of degree 3.

Next we will use a similar argument to derive the limiting complex affine structure for the special Lagrangian fibration of del Pezzo surface of degree 4. We will start from $Y = \mathbb{P}^1 \times \mathbb{P}^1$, D_t smooth anti-canonical divisors of Y converging to an irreducible nodal anti-canonical divisor and $X_t = Y \setminus D_t$. Following the similar argument above, a suitable hyperKähler rotation $\check{X}_t$ can be compactified to a rational elliptic surface $\check{Y}_t$ and $\check{Y}_t$ converging to a rational elliptic surface $\check{Y}_{8'}$ with singular configuration $I_8 I_2 I_1^2$. There exists a $\mathbb{Z}_2 \oplus \mathbb{Z}_2$-action on $\check{Y}_{8'}$. The first copy of the $\mathbb{Z}_2$ is the fibrewise negation and the second copy descends to the

base of the fibration. Again let $r = (1,1) \subseteq \mathbb{Z}_2 \oplus \mathbb{Z}_2$ and consider the elliptic fibration $\check{Y}_{8'}/\langle r \rangle$. The I_8-fibre of $\check{Y}_{8'}$ reduces to an I_4-fibre, the two I_1-fibres are identified under the quotient and the two components of the I_2-fibre are set-wisely fixed, each with two fixed points. The minimal resolution $\check{Y}$ of $\check{Y}_{8'}/\langle r \rangle$ is the unique rational elliptic surface with singular configuration $I_1^* I_4 I_1$, which is the compactification of the mirror Landau-Ginzburg potential of del Pezzo surface of degree 4, viewed as a monotone symplectic manifold. Slightly different from the previous case, $r^* \check{\Omega} = -\check{\Omega}$. From the definition of the complex affine structure and the hyperKähler rotation relation (1.1), this still implies that r sends affine line to affine line with respect to the limiting complex affine structure of the special Lagrangian fibration in $\mathbb{P}^1 \times \mathbb{P}^1$. This leads the following theorem.

Theorem 5.2. *The limiting complex affine structure for del Pezzo surface of degree* 4 *is a* $\mathbb{Z}_2$ *quotient of the limiting complex affine structure of the special Lagrangian in* $\mathbb{P}^1 \times \mathbb{P}^1$. *Explicitly, it is given by the shaded affine subset of* $\mathbb{R}^2$ *in Figure 10 below with* l_1^+ *identified with* l_3^- *and* l_4^+ *identified with* l_4^-.

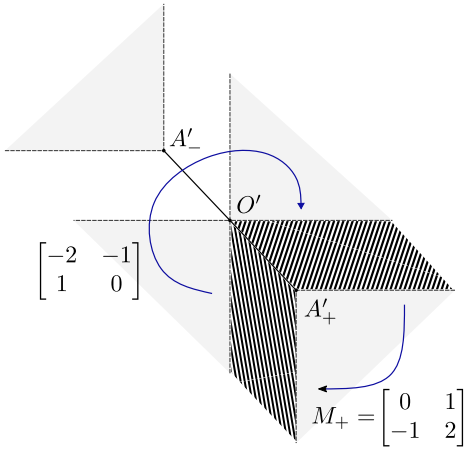

FIGURE 10. The limiting affine structure for del Pezzo surfaces of degree 4.

6. Mirror construction for del Pezzo surfaces using immersed Lagrangians

6.1. **Smoothing of A_n singularities.** Smoothings and resolutions of A_n singularities provide excellent examples of local Calabi-Yau manifolds. The symplectic geometry of A_n smoothings has been well studied by the early work of [58, 60]. SYZ mirror symmetry for A_n singularities was studied in [10, 48]. Rigorously speaking, the previous construction concerns only about Floer theory of smooth SYZ fibers, and points that are mirror to the singular SYZ fibers are missing. In this section, we use the method of [12, 40] to glue in the deformation spaces of immersed nodal spheres in a smoothing of an A_n-singularity. This fills in the corresponding punctures and completes the SYZ mirrors.

Consider a smoothing of A_n surface singularities

$$S = S^{(n)} = \left\{ (X, Y, Z) \in \mathbb{C}^3 : XY = \prod_{i=1}^{n+1} (Z - \epsilon_i) \right\}$$

where $\epsilon_1 < \epsilon_2 < \ldots < \epsilon_{n+1}$ are taken to be real numbers for simplicity. It has a Kähler form restricted from $\mathbb{C}^3$.

We construct Lagrangians in S using symplectic reduction. The $\mathbb{S}^1$-action $(X, Y, Z) \mapsto (e^{i\theta}X, e^{-i\theta}Y, Z)$ is Hamiltonian and has the moment map $\mu = |X|^2 - |Y|^2 : \mathbb{C}^3 \to \mathbb{R}$. The coordinate Z is $\mathbb{S}^1$-invariant and descends to the reduced space $S /\!\!/_a \mathbb{S}^1$. This gives an identification $S /\!\!/_a \mathbb{S}^1 \cong \mathbb{C}$. We will take the level to be $a = 0$. By virtue of the dimension, any curve in $\mathbb{C}$ corresponds to a Lagrangian in S.

Consider a simple loop C in $\mathbb{C}$ which winds around all the points $\epsilon_1, \ldots, \epsilon_{n+1} \in \mathbb{R}$, and is invariant under complex conjugation. It corresponds to a Lagrangian torus

$$L_0 := Z^{-1}(C) \cap \mu^{-1}\{0\} \subset S.$$

For simplicity, let's apply a diffeomorphism ρ on the base $\mathbb{C}$ that commutes with complex conjugation (and in particular preserves the real line) and is equal to identity outside a compact subset, such that $\rho(C)$ is a circle with center lying in the real line.

For each $i = 1, \ldots, n+1$, we take a circle C_i' that satisfies the following requirements.

(1) C_i' passes through the point $\epsilon_i' = \rho(\epsilon_i)$.
(2) The center of C_i' lies in the real line.
(3) C_i' and $\rho(C)$ intersect at two points.
(4) The two strips bounded by $\rho(C)$ and C_i' have the same symplectic area with respect to $(\rho^{-1})^*\omega_{\text{red}}$ (where ω_{red} denotes the reduced symplectic form).

See Figure 11.

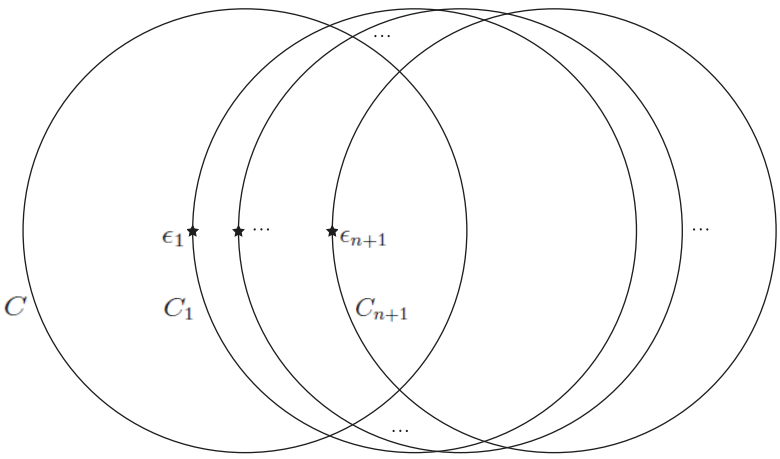

FIGURE 11. The images of the Lagrangians in the reduced space.

Lemma 6.1. *For each $i = 1, \ldots, n+1$, there exists a unique circle C_i' that satisfies the above requirements.*

Proof. Given Condition (1) and (2), the only remaining freedom is the choice of the radius R (in usual Euclidean sense) of C_i'. There exists $a > 0$ such that Condition (3) is satisfied if and only if $R > a$. For $R < R'$, the left strip bounded by $(C_{R'}', C)$ is a subset of that bounded by (C_R', C). Similarly the right strip bounded by $(C_R', C)$is a subset of that bounded by $(C_{R'}', C)$. This implies the symplectic area of the left (or right) strip strictly decreases (or increases resp.) as R increases. At the limit $R = a$ (at which C_i' and C touch at a point), the symplectic area of the right strip is equal to 0; At the limit $R = +\infty$ (at which C_i' is a straight line), the right strip contains an unbounded right half plane, and so has $+\infty$ symplectic area since $(\rho^{-1})^*\omega_{\text{red}} = \omega_{\text{red}}$ (as $\rho = \text{Id}$ outside a compact subset). As a consequence, there exists a unique intermediate value R of the radius such that Condition (4) is satisfied. □

In the above choice, C and $C_i := \rho^{-1}(C_i')$ intersect at two points and bound two strips with the same area under ω_{red}.

Corollary 6.2. *In this setting, each pair of C_i and C_j for $i \neq j$ also intersects at two points and bounds two strips, where the two strips have areas equal to each other under ω_{red}.*

Proof. Without loss of generality, let $\epsilon_i' < \epsilon_j'$ in the real line. We want to show that C_j' does not entirely lie in the disc bounded by C_i', and hence C_i', C_j' intersect at two points and bound two strips. We consider the area form $(\rho^{-1})^*\omega_{\text{red}}$ below.

Suppose this is not true. Let A be the area of each of the two strips bounded by C', C_i'. In this situation, the area of the left strip bounded by C', C_j' is greater than A, and the area of the right strip bounded by C', C_j' is less than A. See the left figure below. This contradicts that the strips bounded by C', C_j' have equal area $\tilde{A}$.

Thus, we are in the situation of the right two figures below. Then

$$\tilde{A} - A = B - D = B'$$

and hence the strips bounded by C_i' and C_j' have equal area $B = B' + D$ under the area form $(\rho^{-1})^*\omega_{\text{red}}$. Applying ρ^{-1}, conclusion follows for $C_i = \rho^{-1}(C_i')$ and $C_j = \rho^{-1}(C_j')$. □

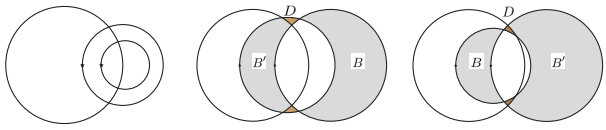

FIGURE 12

We fix a point $p \in \mathbb{R} \subset \mathbb{C}$ in the reduced base, which lies in the common intersection of the discs bounded by the circles C and C_j for $j = 1, \ldots, n+1$. This corresponds to an anti-canonical divisor $Z^{-1}\{p\} \subset S$. We denote the complement by

$$S^\circ := S - Z^{-1}\{p\}.$$

All the Lagrangians we have constructed lie in S°.

It easily follows from the symplectic reduction that:

Lemma 6.3. *For each $i = 1, \dots, n+1$,*

$$L_i := Z^{-1}(C_i) \cap \mu^{-1}\{0\} \subset S^\circ$$

is a Lagrangian immersed sphere with a single nodal point at $X = Y = 0, Z = \epsilon_i$.

The Lagrangian immersions L_i are graded by the holomorphic volume form $dX \wedge dY/(Z-p)$ on S°. Thus, the Maslov index formula of [5, Lemma 3.1] can be applied.

We decorate the Lagrangian torus L_0 with flat $\Lambda_0^\times$-connections. To write them down explicitly, we proceed as follows. First, the fibration $Z : S \to \mathbb{C}$ is trivialized after restricting to the open subset $\{Y \neq 0\} \subset S$. Then we take a basis $\{e_1, e_2\}$ of $\pi_1(L_0) \cong \mathbb{Z}^2$, where e_1 is along the Hamiltonian $\mathbb{S}^1$-action, and e_2 is clockwise along the base circle C. Then the flat connections are parametrized by $z, w \in \Lambda_0^\times$, where z, w are the holonomies along $e_1, e_2 \in \pi_1(L_0)$ respectively. z is the monodromy-invariant direction. We denote these flat connections by $\nabla^{L_0,(z,w)}$.

For the immersed spheres L_i, $i = 1, \dots, n+1$, the self-nodal point gives two immersed generators denoted by U_i and V_i, which correspond to the two branch jumps $q_1 \mapsto q_2$ and $q_2 \mapsto q_1$, where $\{q_1, q_2\} \subset \hat{L}_i$ is the preimage of the nodal point in the normalization $\hat{L}_i \cong \mathbb{S}^2$ of L_i. Using the grading in Lemma 6.3, these generators have degree 1. We shall consider the deformations $b_i = u_i U_i + v_i V_i \in \mathrm{CF}^1(L_i, L_i)$.

Below, we shall follow the construction in [40]. Note that the immersed Lagrangians $\mathbf{L}_i$ are invariant under complex conjugation, and so the argument for weakly unobstructedness still applies. Readers are referred to there for detail.

Lemma 6.4 (Lemma 3.3 of [40])**.** *Consider $L_i \subset S^\circ$ and let $b_i = u_i U_i + v_i V_i \in \mathrm{CF}^1(L_i, L_i)$ with $u_i, v_i \in \Lambda_0$ and $val(u_i v_i) > 0$. We have $m_0^{L_i, b_i} = 0$.*

For $i = 1, \dots, n$, the immersed spheres L_i and L_{i+1} cleanly intersect at two circles (projecting to the two intersection points between C_i and C_{i+1} in the base). Fix a perfect Morse function on each of these circles. The critical points in one of the circles give Floer generators of degree 0 and 1 in $\mathrm{CF}(L_i, L_{i+1})$ (or degree 2 and 1 in $\mathrm{CF}(L_{i+1}, L_i)$); the critical points in the other circle give Floer generators of degree 1 and 2 in $\mathrm{CF}(L_i, L_{i+1})$ (or degree 1 and 0 in $\mathrm{CF}(L_{i+1}, L_i)$). Denote by α_i, β_i the degree zero generators in $\mathrm{CF}(L_i, L_{i+1})$ and $\mathrm{CF}(L_{i+1}, L_i)$ respectively. We find transition between b_i and b_{i+1} such that (α_i, β_i) forms an isomorphism pair:

$$m_1^{b_i, b_{i+1}}(\alpha_i) = 0, m_1^{b_{i+1}, b_i}(\beta_i) = 0; m_2^{b_i, b_{i+1}, b_i}(\alpha_i, \beta_i) = 1_{L_i}, m_2^{b_{i+1}, b_i, b_{i+1}}(\alpha_i, \beta_i) = 1_{L_{i+1}} \tag{6.1}$$

where 1_L denotes the unit of L. Similarly, let α_0 and β_0 denote the degree zero generators in $\mathrm{CF}(L_0, L_1)$ and $\mathrm{CF}(L_1, L_0)$.

Theorem 6.5. *For $i = 1, \dots, n$, α_i is an isomorphism between (L_i, b_i) and (L_{i+1}, b_{i+1}) if $v_i = u_{i+1}^{-1}$ and $u_i = u_{i+1}^2 v_{i+1}$. Moreover, α_0 is an isomorphism between (L_0, b_0) and (L_1, b_1) if $w = u_1$ and $z = u_1 v_1 - 1$.*

Proof. The assertion that α_0 is an isomorphism under the given transition map was proved in [40, Theorem 3.7]. The key ingredient is that

$$m_1^{b_0, b_1}(\alpha_0) = (1 - w u_1^{-1}) X + h(u_1 v_1)(z + 1 - u_1 v_1) Y$$

for a certain series h, where X and Y denote the degree one Floer generators over the base intersection points of β_0 and α_0 respectively. Then $m_1^{b_0,b_1}(\alpha_0) = 0$ gives the gluing formula.

Take a circle of the same radius as C_i and C_{i+1}, whose center lies in the real line, and that passes through a point between ϵ_i and ϵ_{i+1}, see Figure 13. This corresponds to a Lagrangian torus $L_{i,i+1}$. As in the previous paragraph, we have isomorphisms $\alpha^{L_i,L_{i,i+1}}$ and $\alpha^{L_{i+1},L_{i,i+1}}$, under the gluing maps

$$v_i = w^{L_{i,i+1}} = u_{i+1}^{-1},\ u_i v_i = 1 + z^{L_{i,i+1}} = u_{i+1} v_{i+1}.$$

Moreover, we have $m_2(\alpha_i, \alpha^{L_{i+1},L_{i,i+1}}) = \alpha^{L_i,L_{i,i+1}}$: consider the triangle bounded by $L_i, L_{i+1}, L_{i,i+1}$ shaded in Figure 13. The conic fibration trivializes over a neighborhood of this triangle. In particular, it lifts uniquely to a holomorphic triangle in S° with corners passing through the maximum points corresponding to α_i and $\alpha^{L_{i+1},L_{i,i+1}}$. This is the only holomorphic polygon with input corners being α_i and $\alpha^{L_{i+1},L_{i,i+1}}$.

Thus, $\alpha^{L_i,L_{i,i+1}}$ is an isomorphism under the same gluing equation. This gives the claimed transition map. □

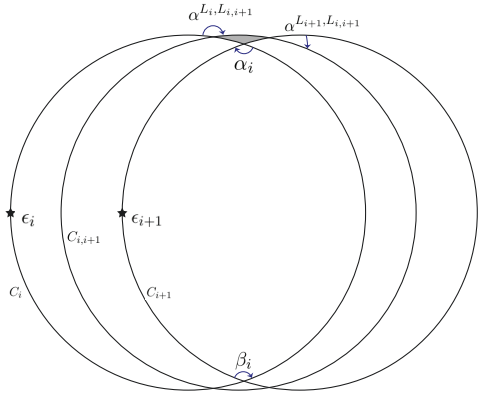

FIGURE 13. The isomorphisms between L_i, L_{i+1}, and the torus $L_{i,i+1}$.

Note that the above gluing equations are the transition maps for a toric resolution of an A_n singularity.

6.2. **Blowing-up over the Novikov field.** To have a better geometric understanding of the above moduli of Lagrangians, we define the following analog of blowing-up over the Novikov ring.

Definition 6.6.

$$\mathbb{P}^1_\Lambda := \left(\Lambda^2 - \{0\}\right)/\Lambda^\times.$$

The blowing up of Λ^2 at a point $(u_0, v_0) \in \Lambda^2$ is defined as

$$\{((u,v), a:b) \in \Lambda^2 \times \mathbb{P}^1_\Lambda : b(u-u_0) = a(v-v_0)\}.$$

The blowing-down map π to Λ^2 is given by forgetting the component $\mathbb{P}^1_\Lambda$. Given a subset $S \subset \Lambda^2$ that contains $(u_0, v_0) \in U + \Lambda^2_+ \subset S$ for some open subset $U \subset \mathbb{C}^2$, the blowing up of S at (u_0, v_0) is defined as $\pi^{-1}(S)$.

We also have the toric resolution of the orbifold singularity at the origin

$$A_{n-1} := \{(u, v, \tilde{z}) \in \Lambda^3 : uv = \tilde{z}^n\} \tag{6.2}$$

over Λ, which is given as a toric surface glued from charts $\Lambda^2_{v_i,u_i}$ by the transitions $v_i = u_{i+1}^{-1}$, $u_i = v_{i+1}u_{i+1}^2$ for $i = 1, \dots, n$ and $n > 1$. (Note that when $n = 1$, it is simply Λ^2.) The blowing down map π is given by $u_1 = u, v_n = v, v_i u_i = \tilde{z}$ for all i. We also have the map $f : A_{n-1} \to \Lambda^2$ forgetting the $\tilde{z}$-coordinate. For a subset $S \subset \Lambda^2$ with $U + \Lambda^2_+ \subset S$ for some open $U \subset \mathbb{C}^2$ containing 0, the blowing up of $f^{-1}(S) \subset A_{n-1}$ at the origin is defined as $\pi^{-1}(f^{-1}(S))$.

Remark 6.7. We have used the notation $\tilde{z}$ for a coordinate in the above definition, to distinguish from the previous holonomy variable z for the torus. They are related by $\tilde{z} = 1 + z$.

Then we have:

Corollary 6.8. *The space $\check{X}_\Lambda$ glued by the unobstructed deformation spaces of the immersed Lagrangians $L_0, \dots, L_{n+1} \subset S^\circ$, where the transition is taken as the solutions to the isomorphism equations for $(\alpha_i, \beta_i) \in \mathrm{CF}^0(L_i, L_{i+1}) \times \mathrm{CF}^0(L_{i+1}, L_i)$, is equal to the resolution of $A_n \cap (\Lambda_0^2 \times (1 + \Lambda_0^\times))$ at 0 when $n > 0$, where A_n is given by Definition 6.6. When $n = 0$, it is equal to $A_0 \cap (\Lambda_0^2 \times (1 + \Lambda_0^\times))$.*

Proof. Note that $(1 + \Lambda_0^\times)^{\frac{1}{n}} = 1 + \Lambda_0^\times$ and $1 + \Lambda_0^\times = \bigcup_{\lambda \in \mathbb{C} - \{1\}} (\lambda + \Lambda_+)$. Consider an element in $1 + \Lambda_0^\times$. Its n-th power lies in $\lambda^n + \Lambda_+$ where $\lambda^n \neq 1$. Thus $(1 + \Lambda_0^\times)^{\frac{1}{n}} \supset 1 + \Lambda_0^\times$. Conversely, consider the n-th root of an element in $\lambda + \Lambda_+$ for $\lambda \neq 1$. If $\lambda = 0$, its n-th root still belongs to $\Lambda_+ \subset 1 + \Lambda_0^\times$; if $\lambda \neq 0$, its n-th root is of the form $\lambda^{1/n} + \Lambda_+$ where $\lambda^{1/n} \neq 1$ (since $\lambda \neq 1$). Thus $(1 + \Lambda_0^\times)^{\frac{1}{n}} \subset 1 + \Lambda_0^\times$.

Then $A_n \cap (\Lambda_0^2 \times (1 + \Lambda_0^\times)) = f^{-1}(S)$, where $S = \{(u, v) \in \Lambda_0^2 : uv \in 1 + \Lambda_0^\times\} \subset \Lambda^2$. It makes sense to talk about the blowing up of $f^{-1}(S)$ by using the above definition.

By Theorem 6.5, the gluing equations for the blowup in Definition 6.6 are satisfied. What remains to show is that the preimage $\pi^{-1}(\Lambda_0^2 \times (1 + \Lambda_0^\times))$ (where π is the blowing down map) is equal to the union of the charts $(\Lambda_0^\times)^2$ of L_0 and $\{(u_i, v_i) \in \Lambda_0^2 : \mathrm{val}\,(u_i v_i) > 0\}$ of L_i for $i = 1, \dots, n + 1$.

First, we show that the union of charts is a subset of $\pi^{-1}(\Lambda_0^2 \times (1 + \Lambda_0^\times))$. It is easy to see that for $(u, v, \tilde{z}) \in \pi((\Lambda_0^\times)^2_{u_1, \tilde{z}-1})$ (where $(\Lambda_0^\times)^2_{u_1,\tilde{z}-1}$ is the chart for L_0), $u = u_1 \in \Lambda_0^\times \subset \Lambda_0$, $\tilde{z} \in 1 + \Lambda_0^\times$, and $v = u^{-1}\tilde{z}^n \in \Lambda_0$. Also for $(u, v, \tilde{z}) \in \pi(\{(u_i, v_i) \in \Lambda_0^2 : \mathrm{val}\,(u_i v_i) > 0\})$, $\tilde{z} = u_i v_i \in \Lambda_+ \subset 1 + \Lambda_0^\times$; moreover, since both $u = u_1$ and $v = v_{n+1}$ are of the form $u_i^r v_i^s$ for $r, s \in \mathbb{Z}_{\geq 0}$, we have $u, v \in \Lambda_0$. Thus we see that the union of charts is a subset of $\pi^{-1}(\Lambda_0^2 \times (1 + \Lambda_0^\times))$.

To show the converse, first we prove the statement for $n = 0$. Namely, the union of the chart $(\Lambda_0^\times)^2_{u_1,\tilde{z}-1}$ of L_0 with the chart $\{(u_1, v_1) \in \Lambda_0^2 : \mathrm{val}\,(u_1 v_1) > 0\}$ of L_1 is equal to $\{(u_1, v_1, \tilde{z}) \in \Lambda_0^2 \times (1 + \Lambda_0^\times) : u_1 v_1 = \tilde{z}\}$. The subset relation is known from the previous paragraph. Conversely, $\mathrm{val}\,(u_1 v_1)$ is either positive or zero. If it is positive, the point belongs

to the chart of L_1. If it is zero, then $u_1 \in \Lambda_0^\times$, and hence the point belongs to the chart of L_0.

Note that the above statement is symmetric with respect to u_1 and v_1. This means the union of $(\Lambda_0^\times)^2_{v_1,\tilde{z}^{-1}}$ with $\{(u_1,v_1) \in \Lambda_0^2 : \mathrm{val}\,(u_1v_1) > 0\}$ is equal to $\{(u_1,v_1,\tilde{z}) \in \Lambda_0^2 \times (1+\Lambda_0^\times) : u_1v_1 = \tilde{z}\}$. Note that by $u_2 = v_1^{-1}$, we have $(\Lambda_0^\times)^2_{v_1,\tilde{z}^{-1}} = (\Lambda_0^\times)^2_{u_2,\tilde{z}^{-1}}$. Proceeding in the same way, the union of $(\Lambda_0^\times)^2_{u_2,\tilde{z}^{-1}}$ and $\{(u_2,v_2) \in \Lambda_0^2 : \mathrm{val}\,(u_2v_2) > 0\}$ gives $\{(u_2,v_2,\tilde{z}) \in \Lambda_0^2 \times (1+\Lambda_0^\times) : u_2v_2 = \tilde{z}\}$. Inductively, we conclude that the union of the charts of L_i for $i = 0,\dots,n+1$ is equal to the union of $\{(u_j,v_j,\tilde{z}) \in \Lambda_0^2 \times (1+\Lambda_0^\times) : u_jv_j = \tilde{z}\}$ for $j = 1,\dots,n+1$.

Now we are ready to show the converse for general n. Given $(u,v,\tilde{z}) \in \pi^{-1}(\Lambda_0^2 \times (1+\Lambda_0^\times))$, we need to show that it belongs to the union of $\{(u_j,v_j,\tilde{z}) \in \Lambda_0^2 \times (1+\Lambda_0^\times) : u_jv_j = \tilde{z}\}$ for $j = 1,\dots,n+1$. We already know that $u_1 = u \in \Lambda_0$. If $v_1 \in \Lambda_0$, we are done. Otherwise, $u_2 = v_1^{-1} \in \Lambda_0$. If $v_2 \in \Lambda_0$, then we are done. Inductively, either we get that the point belongs to $\{(u_j,v_j,\tilde{z}) \in \Lambda_0^2 \times (1+\Lambda_0^\times) : u_jv_j = \tilde{z}\}$ for some $j = 1,\dots,n$, or we get $u_{n+1} \in \Lambda_0$. Since $v_{n+1} = v \in \Lambda_0$, the point belongs to $\{(u_{n+1},v_{n+1},\tilde{z}) \in \Lambda_0^2 \times (1+\Lambda_0^\times) : u_{n+1}v_{n+1} = \tilde{z}\}$ in this case. □

In the above, the local charts are $\{(u,v,\tilde{z}) \in \Lambda_0^2 \times (1+\Lambda_0^\times) : uv = \tilde{z}\}$. They turn out to have a very nice relation with an open subset over $\mathbb{C}$:

Proposition 6.9. $\{(u,v,\tilde{z}) \in \Lambda_0^2 \times (1+\Lambda_0^\times) : uv = \tilde{z}\} = (\mathbb{C}^2 - \{uv = 1\}) + \Lambda_+^2$.

Proof. The proof is by stratifying both sides into two pieces: the left hand side is equal to

$$\{\mathrm{val}\,uv > 0\} \sqcup \{\mathrm{val}\,u = \mathrm{val}\,v = 0, uv \in (\mathbb{C} - \{0,1\}) + \Lambda_+\}$$

and the right hand side is equal to

$$\left(\{uv = 0\} + \Lambda_+^2\right) \sqcup \left(\{uv \neq 0,1\} + \Lambda_+^2\right).$$

To verify that $\{\mathrm{val}\,uv > 0\} = (\{uv = 0\} + \Lambda_+^2)$, we can further stratify to three pieces

$$\{\mathrm{val}\,u \text{ and } \mathrm{val}\,v > 0\} \sqcup \{\mathrm{val}\,u > 0 \text{ and } \mathrm{val}\,v = 0\} \sqcup \{\mathrm{val}\,v > 0 \text{ and } \mathrm{val}\,u = 0\}$$

and

$$\left(\{u = v = 0\} + \Lambda_+^2\right) \sqcup \left(\{u = 0 \text{ and } v \in \mathbb{C}^\times\} + \Lambda_+^2\right) \sqcup \left(\{v = 0 \text{ and } u \in \mathbb{C}^\times\} + \Lambda_+^2\right)$$

respectively. Then it is easy to see that they are equal to each other.

To verify that $\{\mathrm{val}\,u = \mathrm{val}\,v = 0, uv \in (\mathbb{C} - \{0,1\}) + \Lambda_+\} = (\{uv \neq 0,1\} + \Lambda_+^2)$, one can check that both sides consist of elements (u,v) of the form $u = u_0 + u_+, v = v_0 + v_+$, where $u_0, v_0 \in \mathbb{C}^\times$ with $u_0v_0 \neq 1$, and $u_+, v_+ \in \Lambda_+$. □

Remark 6.10. The proof shows that the glued mirror from (L_i, b_i) for $i = 0,\dots,n+1$ in the smoothing $S^{(n)}$ is equal to the union of these charts $((\mathbb{C}^2 - \{uv = 1\}) + \Lambda_+^2) \subset \Lambda^2$. Taking the intersection of each chart with $\mathbb{C}^2 \subset \Lambda^2$, we get the complex surface $\{(u_j,v_j,\tilde{z}) \in \mathbb{C}^2 \times (\{1\} + \mathbb{C}^\times) : u_jv_j = \tilde{z}\}$, which is equal to the usual $\mathbb{C}$-valued A_n-resolution minus the anti-canonical divisor with local description $u_jv_j = 1$.

The $\mathbb{C}$-valued mirror is glued from the Clifford torus L_0 with flat $\mathbb{C}^\times$-connections (for $\tilde{z} \in 1 + \mathbb{C}^\times$ and $u_1 \in \mathbb{C}^\times$), and the immersed sphere L_i (for $i = 1,\dots,n$) with boundary deformations $u_iU_i + v_iV_i$ with $u_iv_i = 0$.

As a result, resolutions of an A_n-singularity are mirror to smoothings of the A_n-singularity. By the construction in [12], there exists an A_∞ functor from the Fukaya category of S° to the category of twisted complexes over $\check{X}_\Lambda$. In this sense, the local A_n-singularity is self-mirror.

The relationship between Λ_0 and $\mathbb{C}$ can be formulated more systematically by defining the following.

Definition 6.11. Given a complex manifold M, its extension over the Novikov ring, denoted by $M+\Lambda_+^n$, is defined as the union of charts $U+\Lambda_+^n$ glued by the same transition functions of M, where U are charts of M. For an analytic subset $Z \subset M$, its extension over the Novikov ring, denoted by $Z+\Lambda_+^n$, is the union of $Z_p+\Lambda_+^n$, where $Z_p \subset U_p$ is the neighborhood of p in Z lying in a local chart $U_p \subset \mathbb{C}^n$ of M and is given as the zero locus of a (finite) set of complex analytic functions.

The above is well-defined since for an analytic function f, $f(z) \in f(z_0)+\Lambda_+$ where $z \in z_0+\Lambda_+$ and $z_0 \in \mathbb{C}$.

Using the above definition, Proposition 6.9, and Corollary 6.8, we get the following.

Corollary 6.12. *The resolution of $A_n \cap (\Lambda_0^2 \times (1+\Lambda_0^\times))$ is equal to $\hat{A}_n+\Lambda_+^2$, where $\hat{A}_n$ is the resolution of $\{(u,v,\tilde{z}) \in \mathbb{C}^2 \times (\mathbb{C}-\{1\}) : uv = \tilde{z}^n\}$ over $\mathbb{C}$.*

Similarly,

Proposition 6.13. *For an open subset $U \subset \mathbb{C}^2$ with $(u_0,v_0) \in U$, the blowing up of $U+\Lambda_+^2$ (over Λ) at (u_0,v_0) is equal to $\hat{U}+\Lambda_+^2$ where $\hat{U}$ denotes the blowing up of U at (u_0,v_0) (over $\mathbb{C}$).*

For the purpose of the next section, it is useful to have another description of the above total space of an A_n-resolution in terms of the usual repeated blowing-up at a point.

Proposition 6.14. *The resolution $\check{X}_\Lambda$ of $A_n \cap (\Lambda_0^2 \times (1+\Lambda_0^\times))$ (where the resolution does nothing for $n=0$) is equal to M' constructed as follows. Take the blowing-up of $\Lambda_0 \times (1+\Lambda_0^\times) = (\mathbb{C}^2_{u,\tilde{z}} - \{\tilde{z}=1\}) + \Lambda_+^2$ at $(u,\tilde{z}) \in (0,0)$, and repeatedly take the blowing-up again at a point in the new exceptional curve n times, so that we have $(n+1)$ exceptional curves in total. M' is defined to be the complement of $(Z'+\Lambda_+^2)$, where Z' (over $\mathbb{C}$) is the strict transform of the $\tilde{z}$-axis $\{u=0\} \subset \mathbb{C}^2_{u,\tilde{z}} - \{\tilde{z}=1\}$.*

Remark 6.15. We have a global analytic function $\tilde{z} : \check{X}_\Lambda \to \Lambda - \{1\}$. By taking $\tilde{z}=0$ (that is, the holonomy variable $z=-1+\tilde{z}=-1$) and gluing the valuation images of $(\mathrm{val}(u_i), \mathrm{val}(v_i))$ in all the charts, we get the 'skeleton' as shown in Figure 14.

6.3. **Application to Del Pezzo surfaces of degree higher than two.** Let's consider toric Gorenstein Fano surfaces. Their smoothings give del Pezzo surfaces of degree ≥ 3. A_n singularities occur at the toric fixed points. The gluing method using Fukaya isomorphisms from the last subsection can be used to construct their Landau–Ginzburg mirrors. The mirror pairs we construct in this way are summarized by Figure 15.

Take a toric Gorenstein Fano surface M_0 equipped with a toric Kähler form, such that its moment-map polytope is integral and contains the origin as the unique interior lattice point.

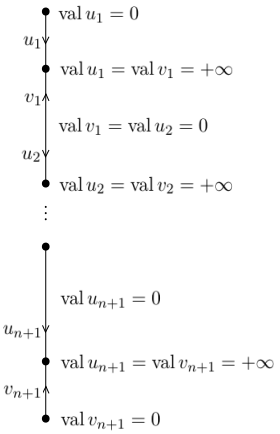

FIGURE 14. A skeleton of $\check{X}$ obtained by taking valuation image.

Let $\mathbf{L}_0$ be the moment map torus fibre over the origin. Then M_0 is a monotone symplectic manifold, and $\mathbf{L}_0$ is a monotone Lagrangian torus.

Let's denote by F the set of toric fixed points. Each $p \in F$ corresponds to a maximal cone of the fan, whose dual cone gives a toric chart containing the fixed point. The toric chart is given by

$$S_0 := \{(X, Y, Z) \in \mathbb{C}^3 : XY = Z^{n+1}\}$$

when the toric fixed point 0 is an A_n singularity (and $n = 0$ if it is a smooth point).

If necessary (when $n \geq 1$), we take a smoothing family $S_\epsilon := \{(X, Y, Z) \in \mathbb{C}^3 : XY = \prod_{i=1}^{n+1}(Z - \epsilon_i)\}$ as in the last subsection. This is a family over $\mathbb{C}^{n+1}$, where ϵ lives. Such a smoothing is $\mathbb{S}^1$-equivariant, where $\mathbb{S}^1$ acts by $(X, Y, Z) \mapsto (e^{i\theta}X, e^{-i\theta}Y, Z)$. This can be understood as an $\mathbb{S}^1$-equivariant symplectic fibration over $\mathbb{C}^{n+1}$ (where S_ϵ is equipped with the restricted standard symplectic form of $\mathbb{C}^3$). By symplectic parallel transport, $U_\epsilon - \bigcup_{i=1}^n \mathbb{S}_i$ is symplectomorphic to $U_0 - \{0\}$, where $\mathbb{S}_i$ are the vanishing spheres whose images in the reduced base are line segments in the real line joining $Z = \epsilon_i$ and $Z = \epsilon_{i+1}$; U_ϵ and U_0 are certain $\mathbb{S}^1$-invariant neighborhoods of $\bigcup_{i=1}^n \mathbb{S}_i \subset S_\epsilon$ and $0 \in S_0$ respectively. Moreover, by the Moser argument, $(S_0, \omega_{M_0}) - \{0\}$ is symplectomorphic to an open subset of $(S_0, \omega_{\mathbb{C}^3}) - \{0\}$. Combining these, we have an $\mathbb{S}^1$-equivariant symplectomorphism between $(U_\epsilon - \bigcup_{i=1}^n \mathbb{S}_i, \omega_{\mathbb{C}^3})$ and $(S_0 - \{0\}, \omega_{M_0})$ for some neighborhoods $U_\epsilon \subset S_\epsilon$.

By gluing the patches U_ϵ and $M_0 - \{0\}$ using the above symplectomorphism, we obtain a (partial) symplectic smoothing of M_0. Repeating the surgery at all singular toric fixed points, we obtain a symplectic del Pezzo surface which is denoted by X.

Similarly to the $\mathbb{S}^1$-equivariance, we also have $\mathbb{Z}_2$-equivariance for the anti-symplectic involution on S_ϵ: $(X, Y, Z) \mapsto (\bar{Y}, \bar{X}, \bar{Z})$, and the above symplectomorphisms are made to be $\mathbb{Z}_2$-equivariant.

In particular, the monotone Lagrangian torus $\mathbf{L}_0 \subset (S_0, \omega_{M_0}) - \{0\}$ is sent via the symplectomorphism to a corresponding Lagrangian torus, which is denoted by L_0, in $U_\epsilon - \bigcup_{i=1}^n \mathbb{S}_i \subset X$. L_0 is invariant under $\mathbb{S}^1$ and the anti-symplectic involution. This matches the setting for L_0 in the last subsection. Thus for the i-th toric fixed point (ordered

counterclockwise around the moment-map polytope), which is an A_{n_i}-singularity for $n_i \geq 0$, the construction gives Lagrangian immersed spheres $\mathbf{L}_{i,k}$ for $k = 1, \ldots, n_i + 1$ in X.

Lemma 6.16. *X and $\mathbf{L}_0 \subset X$ are monotone.*

Proof. The curve classes in $\pi_2(M_0)$ have symplectic areas and Maslov indices unchanged under smoothing. Moreover, the matching spheres in the smoothing have both Maslov index and area being zero. Thus X is still monotone.

Similarly, the basic disc classes in $\pi_2(M_0, \mathbf{L}_0)$ have areas and Maslov indices unchanged after smoothing, and hence $\mathbf{L}_0$ remains monotone. □

Lemma 6.17. *$\mathbf{L}_0$ and the immersed Lagrangians $\mathbf{L}_{i,j}$ have minimal Maslov index two. In particular m_0^b is proportional to the unit.*

Proof. We have a symplectomorphism $M_0 - \{\text{toric fixed points}\} \cong X - \{\text{vanishing spheres}\}$. In $M_0 - \{\text{toric fixed points}\}$, we already know that $\mathbf{L}_0$ has minimal Maslov index two, since it is special with respect to the toric meromorphic volume form. In the smoothing of each toric chart around a singular fixed point, the non-constant holomorphic discs bounded by $\mathbf{L}_0$ have Maslov indices greater than zero. Since any disc class bounded by $\mathbf{L}_0$ is a linear combination of disc classes in the charts, $\mathbf{L}_0$ has minimal Maslov index two.

Holomorphic polygon classes bounded by the immersed Lagrangian $\mathbf{L}_{i,j}$ is a sum of non-constant holomorphic disc classes corresponding to those of $\mathbf{L}_0$ with constant polygon classes that has Maslov index zero. Thus $\mathbf{L}_{i,j}$ also has minimal Maslov index two.

m_0^b has degree two. Since the minimal Maslov index is two, the degree of an output in m_0^b cannot be bigger than zero, which can only be the unit. □

By the isomorphisms between the Lagrangian objects $\mathbf{L}_0$ and $\mathbf{L}_{i,j}$ for $p \in F$ and $j = 1, \ldots, n_i + 1$ given in the last subsection, we obtain a manifold glued from the formal deformation spaces of the Lagrangians. We call it the Floer-theoretical mirror space.

Let $\check{\Delta}$ be the polar dual polytope of Δ, and $X_{\check{\Delta}}$ be the corresponding toric variety over $\mathbb{C}$. For each toric chart corresponding to a fixed point of $X_{\check{\Delta}}$, we have the points $(-1, 0)$ and $(0, -1)$ lying in the toric divisors, which are invariant under toric change of coordinates. We call these special points in $X_{\check{\Delta}}$. It is easy to see that there is a natural one-to-one correspondence between the collection of special points in $X_{\check{\Delta}}$ and the toric fixed points of X_Δ.

We consider the toric variety over Λ, $X_{\check{\Delta}} + \Lambda_+^2$ (see Definition 6.11).

Remark 6.18. A toric variety over Λ can also be defined as a GIT quotient of Λ^n over $\Lambda^\times$ (like $\mathbb{P}^1_\Lambda$ in Definition 6.6). When the corresponding fan picture is complete, it agrees with the extension of the toric variety over the Novikov ring.

To make notations precise, recall that the toric fixed points of X_Δ are labeled by i. Toric fixed points of X_Δ correspond to toric prime divisors of $X_{\check{\Delta}}$. We denote the toric coordinates on these toric divisors by z_i. The special points in the divisors are $z_i = -1$.

Theorem 6.19. *The Floer-theoretical mirror space is equal to $\check{X}_\Lambda = \check{X} + \Lambda_+^2$, where $\check{X}$ is given as follows. First, we take the (multiple) blowing up of the toric variety $X_{\check{\Delta}}$ at every special point $z_i = -1$ in the i-th toric divisor for $(n_i + 1)$-times (where $n_i + 1$ is the*

multiplicity of the i-th toric fixed point of X_Δ). Then we define $\check{X}$ to be the complement of the strict transform of all the toric divisors of $X_{\check{\Delta}}$.

Proof. By Corollary 6.8 and Proposition 6.14, fixing i, the deformation spaces of $\mathbf{L}_0$ and $\mathbf{L}_{i,j}$ for $j = 1, \dots, n_i+1$ glue up to the Novikov extension of a multiple blowing up of $\mathbb{C}^\times_{z_i} \times \mathbb{C}_{u_i}$ at $(u_i, z_i) = (0, -1)$, with the strict transform of the z_i-axis removed, where z_i is the holonomy variable corresponding to the vanishing cycles of $\mathbf{L}_{i,j}$. (In the notation of the previous section, $z_i = \tilde{z}_i - 1$.) The direction of z_i determines the toric compactification $\mathbb{C}^\times_{z_i} \times \mathbb{C}_{u_i}$ of $(\mathbb{C}^\times)^2$ (which corresponds to adding a ray dual to z_i in the fan picture). These holonomy directions are obtained by taking the orthogonal complement of $\xi_i + \eta_i$, where ξ_i and η_i are the edge directions of the i-th corner of the moment-map polytope of M_0. From this, we see that the charts $\mathbb{C}^\times_{z_i} \times \mathbb{C}_{u_i}$ glue to the toric variety $X_{\check{\Delta}} - \{\text{toric fixed points of } X_{\check{\Delta}}\}$. It follows that the entire space glued from $\mathbf{L}_0$ and $\mathbf{L}_{i,j}$ for all i, j is equal to $\check{X} + \Lambda_+^2$. □

Remark 6.20. $\check{X}_\Lambda$ can also be constructed by taking the (multiple) blowing up of $X_{\check{\Delta}} + \Lambda_+^2$ using Definition 6.6, and then taking the complement of $\hat{D} + \Lambda_+^2$ for all the toric divisors $D \subset X_{\check{\Delta}}$ (where $\hat{D}$ denotes the strict transform).

The coordinates z_i form analytic maps $\check{X}_\Lambda \to \mathbb{P}^1_\Lambda$ (since the strict transform of the toric divisors, and in particular the toric fixed points, have been removed). The union of the valuation images of $(u_{i,j}, v_{i,j})$ on $z_i = -1$ form a skeleton. See Figure 16 for an example.

By Theorem 6.19, the space $\widehat{X_{\check{\Delta}}} - D_{\check{\Delta}}$ is obtained by gluing according to isomorphisms of Lagrangians. Thus the disc potential W_{L_0} of L_0 must extend as a well-defined function to the whole $\widehat{X_{\check{\Delta}}} - D_{\check{\Delta}}$.

Corollary 6.21. *The disc potential $W_{\mathbf{L}_0}$ extends as a well-defined function over $\widehat{X_{\check{\Delta}}} - D_{\check{\Delta}}$.*

Let $v_1, \dots, v_p$ be the primitive inward normal vectors to the facets of the moment-map polytope of the toric variety M_0, which are ordered counterclockwisely. (Thus (v_i, v_{i+1}) agrees with the standard orientation of the plane.) The multiplicities at toric fixed points are equal to $n_i = \det(v_i, v_{i+1})$. The toric fixed points are A_{n_i-1}-singularities. Then $u_{i,j} = (jv_i + (n_i - j)v_{i+1})/n_i$ for $j \in [2, n_i - 1] \cap \mathbb{Z}$ are integral vectors.

Proposition 6.22. *The disc potential $W_{\mathbf{L}_0}$ is equal to*

$$W_{\mathbf{L}_0} = \sum_i z^{v_i} + \sum_i \sum_{j=2}^{n_i-1} \binom{n_i}{j} z^{u_{i,j}}.$$

Proof. The disc potential for $\mathbf{L}_0$ in the A_{n_i}-smoothing of the i-th toric chart corresponding to (v_i, v_{i+1}) is equal to

$$z^{v_i} + z^{v_{i+1}} + \sum_{j=2}^{n_i-1} \binom{n_i}{j} z^{u_{i,j}}.$$

$$z^{v_i}(1 + z^{u_{i,2}-v_i})^{n_i}$$

Since $\mathbf{L}_0$ is monotone, the disc potential is invariant under deformation of complex structures [20]. We show below that a Maslov-two holomorphic disc bounded by $\mathbf{L}_0$ must be

entirely contained in one of the charts. Then it follows that the disc potential of $\mathbf{L}_0$ in X is a sum of the potentials in the various charts.

Let's choose an embedding of the open torus orbit $(\mathbb{C}^\times)^2$ of the toric degeneration to X, whose complement C is a union of Lagrangian vanishing spheres together with chosen branches of degenerate conics in the charts. In dimension two, C represents the anti-canonical class. This can be easily seen by deforming X to a resolution of singularities in which the vanishing spheres become holomorphic. It follows that a holomorphic disc of Maslov-index two intersects the anti-canonical class C once. Thus it is contained in a chart. □

Explicit expressions of W_{L_0} are given in Table 1. Comparing to Figure 15, for each dP_n, we only write down the disc potential for the monotone torus associated to the toric variety shown as the first figure, since the others can be obtained via wall-crossing. They give different realizations of the *same mirror space* as the complement of a (non-toric) blowing-up of a toric variety.

Example 6.23. *Consider dP_4' obtained as smoothings of the two toric varieties shown in Figure 15. The disc potential associated to the first one is equal to*

$$W_0 = xy + xy^{-1} + x^{-1}y + x^{-1}y^{-1} + 2(x + y + x^{-1} + y^{-1}).$$

It is related to the disc potential associated to the second one by wall-crossing

$$y' = y(x + x^{-1} + 2);\ x' = x.$$

The potential becomes

$$\begin{aligned}&(x + x^{-1} + 2)y^{-1} + 2x^{-1} + 2x + y(x + x^{-1} + 2)\\ =&(x' + (x')^{-1} + 2)^2(y')^{-1} + 2x^{-1} + 2x + y'\\ =&(x')^2(y')^{-1} + (x')^{-2}(y')^{-1} + y' + 2x' + 2(x')^{-1} + 4\left(x'(y')^{-1} + (x')^{-1}(y')^{-1}\right) + 6(y')^{-1}.\end{aligned}$$

The coordinate change between y' and y is composed of crossing two parallel walls in the A_1 configuration. Namely, $y' = yx^{-1}(1 + x)^2 = y(x + x^{-1} + 2)$.

dP_9	$W_0 = x + y + (xy)^{-1}$
dP_8	$W_0 = x + y + y^{-1} + x^{-1}y^{-1}$
dP_8'	$W_0 = x + y + x^{-1} + y^{-1}$
dP_7	$W_0 = x + y + x^{-1} + y^{-1} + x^{-1}y^{-1}$
dP_6	$W_0 = x + y + xy + x^{-1} + y^{-1} + x^{-1}y^{-1}$
dP_5	$W_0 = xy + x^{-1}y + xy^{-1} + x^{-1} + y^{-1} + 2x + 2y$
dP_4	$W_0 = xy + xy^{-1} + y^{-1} + x^{-2}y + 2x + 2x^{-1} + 3y + 3x^{-1}y$
dP_4'	$W_0 = xy + xy^{-1} + x^{-1}y + x^{-1}y^{-1} + 2(x + y + x^{-1} + y^{-1})$
dP_3	$W_0 = xy + x^{-2}y + xy^{-2} + 3(x + xy^{-1} + y + x^{-1}y + x^{-1} + y^{-1})$

TABLE 1. The disc potentials of toric monotone tori in del Pezzo surfaces.

Appendix A. Construction of rational elliptic surfaces with an I_d fibre and trivial periods

In the appendix, by reverse engineering the algorithm in proof of [30, Proposition 1.3], we construct the rational surface with an I_d fibre and trivial period explicitly below.

The del Pezzo surfaces dP_d of degree $d = 6, 7, 8, 9$ are toric varieties. Applying Batyrev's toric mirror construction and taking a further blow-up yield the desired rational elliptic surfaces. We thus focus on the case $1 \leq d \leq 5$.

A.1. $d = 5$**.** Recall that the del Pezzo surface of degree seven dP_7 is a toric surface whose fan is generated by $(-1,0),(0,-1),(1,0),(1,1),(0,1)$. Denote by D_i, $i = 1,\dots 5$, the corresponding toric divisors. Then the del Pezzo surface of degree five Y_5 can be realized as the blow-up of dP_7 at the point "-1" on the toric divisors D_1 and D_2. Then $\check{Y}_e$ is the blow-up along the preimage of "-1" on each of D_i in Y_t and $\check{D}_e$ is the proper transform of $\sum_{i=1}^5 D_i$.

A.2. $d = 4$**.** We start with the toric variety $\mathbf{P}^1 \times \mathbf{P}^1$. Let D_i, $i = 1,\dots 4$, be the irreducible toric boundaries. Let Y_4' be the blow up of $\mathbf{P}^1 \times \mathbf{P}^1$ at "-1" on each D_i. Then $\check{Y}_e$ is the blow up of the intersection of the exceptional divisors with the proper transform of D_i. Then $\check{Y}$ is a blow-up of $\mathbf{P}^1 \times \mathbf{P}^1$ at eight points and thus a rational elliptic surface. The I_4 fibre is the proper transform of $\sum_i D_i$. In this case the singular configuration is $I_1^* I_4 I_1$.

A.3. $d = 3$**.** We begin with $\mathbf{P}^2$ and irreducible toric boundaries D_i, $i = 1, 2, 3$. Let Y_3' be the blow-up of $\mathbf{P}^2$ along "-1" on each toric boundary. Let Y_3'' be the blow-up of Y_3' along the intersection of the exceptional divisors with the proper transform of D_i. Then $\check{Y}_e$ is the blow-up of Y_3'' along the intersections of the exceptional divisors of $Y_3'' \to Y_3'$ and the proper transform of D_i. The boundary divisor is then the proper transform of D_i to $\check{Y}_e$. Then $\check{Y}_e$ is the blow up of $\mathbf{P}^2$ at nine points and thus a rational elliptic surface. In this case, the singular configuration is $\mathrm{IV}^*\mathrm{I}_3\mathrm{I}_1$.

A.4. $d = 2$**.** Recall that the rays in the fan of $\mathbf{P}^1 \times \mathbf{P}^1$ are generated by $(1,0)$, $(0,1)$, $(-1,0)$, $(0,-1)$. Denote by D_i, $i = 1,\dots,4$, the corresponding toric divisor. Let Y_2' be obtained from blowing up $\mathbf{P}^1 \times \mathbf{P}^1$ at "-1" on D_2 and D_4 respectively and then contract the proper transform of D_2, D_4. Then Y_2' is a minimal rational surface of second Betti number 2. Since the proper transform of $\{-1\} \times \mathbf{P}^1 \subseteq \mathbf{P}^1 \times \mathbf{P}^1$ (which is homologous to D_1 or D_3) is a (-2)-curve, we have $Y_2' \cong \mathbb{F}_2$. Then $\check{Y}_2$ is the four-time iterated blow up at (-1) of D_1, D_3. Then $\check{Y}_e$ is the blow up of Y_2' at the points corresponding to -1 on the proper transform of D_2, D_4. $\check{D}_e$ is the proper transform of D_1, D_3. Then $\check{Y}_2$ is a rational elliptic surface with singular configuration $\mathrm{III}^*\mathrm{I}_2\mathrm{I}_1$, where the component of the III^* fibre with multiplicity 4 is the proper transform of $\mathbf{P}^1 \times \{-1\}$ from $\mathbf{P}^1 \times \mathbf{P}^1$, which is homologous to D_2, D_4.

A.5. $d = 1$**.** Let (x,t) and (z,s) be two charts of $\mathcal{O}_{\mathbf{P}^1}(3)$ such that $x = 1/z, t = x^3 s$. Let L be the compactification of the curve locally defined by $\{t + (x+1)^3 = 0\}$ in the Hirzebruch surface $\mathbb{F}_3 \cong \mathbb{P}(\mathcal{O} \oplus \mathcal{O}_{\mathbf{P}^1}(3))$. Then L intersect two toric boundary fibres at -1 and is tangent to the $(+3)$-toric boundary divisor at -1 with multiplicity 3. Blowing up the intersection of L with the two toric boundary fibres and blow down the two fibres and the original unique -3 curve leads to $\mathbf{P}^2$. The proper transform of the original $(+3)$-toric boundary divisor is a

nodal cubic C and is tangent to the proper transform of L with multiplicity 3 at p. Then $\check{Y}_1$ is the nine-times successive blow up at the point corresponding to p on the proper transform of C. The proper transform of L on $\check{Y}_1$ is the component of the II^* fibre with multiplicity 3 and adjacent to the unique component of multiplicity 6.

Appendix B. Proof of Lemma 4.12

We retain the notation in §4. We can compute

$$\mathrm{Im}\left(\int_{\partial b(q)} \iota_{\partial/\partial q}\check{\Omega}\right) < 0 \text{ for } q \in (-4, 0).$$

To prove the lemma, it suffices to show that there exists a constant $\kappa > 0$ such that

$$\mathrm{Im}\left(\int_{-\partial a(q)} \iota_{\mathrm{i}\partial/\partial q}\check{\Omega}\right) \geq \frac{\kappa}{|q|}, \text{ for all } q \text{ large.} \tag{B.1}$$

Let p_1 and p_2 be ramification points such that $\mathrm{Re}\, p_1 > 0$, $\mathrm{Im}\, p_1 > 0$ and $\mathrm{Re}\, p_2 > 0$, $\mathrm{Im}\, p_2 < 0$. (p_1 and p_2 are roots of $t^2 - (2+q)t + 1 = 0$.) We may write $p_1 = R\exp(\mathrm{i}\theta_0)$ and $p_2 = \epsilon\exp(-\mathrm{i}\theta_0)$ where $R = |p_1|$ and $\epsilon = |p_2|$. Note that R, ϵ, and θ_0 indeed depend on q but we shall drop out q in the notation for simplicity. Let $\gamma_{1,1}$ be a circular arc of radius R connecting p_1 and the positive real axis, $\gamma_{1,2}$ be the line segment connecting ϵ and R on the positive real axis, and $\gamma_{1,3}$ be a circular arc of radius ϵ connecting p_2 and the positive real axis (cf. Figure 18). We can deform γ_1 into $\gamma_{1,1} \cup \gamma_{1,2} \cup \gamma_{1,3}$. Note that

$$\sqrt{(t_2^2 + 1 - qt_2)^2 - 4t_2^2} = t_2 \cdot \sqrt{(t_2 + t_2^{-1} - q)^2 - 4}.$$

on $\gamma_{1,1} \cup \gamma_{1,2} \cup \gamma_{1,3}$. We shall compute

$$\int_{\gamma_{1,j}} \frac{\mathrm{d}t_2}{\sqrt{(t_2^2 + 1 - qt_2)^2 - 4t_2^2}} = \int_{\gamma_{1,j}} \frac{1}{\sqrt{(t_2 + t_2^{-1} - q)^2 - 4}} \frac{\mathrm{d}t_2}{t_2}.$$

Lemma B.1. *For $j = 1, 2, 3$, we have*

$$\mathrm{Im}\left(\int_{\gamma_{1,j}} \frac{1}{\sqrt{(t_2 + t_2^{-1} - q)^2 - 4}} \frac{\mathrm{d}t_2}{t_2}\right) \geq 0.$$

Proof. We claim that

$$\mathrm{Im}\left((t_2 + t_2^{-1} - q)^2 - 4\right) \leq 0, \text{ for } t_2 \in \gamma_{1,j}. \tag{B.2}$$

The lemma immediately follows from the claim.

For $j = 2$, (B.2) is true since $t_2 \in \mathbb{R}_+$ and $q \in \mathrm{i}\cdot\mathbb{R}_+$. Let us consider the case $j = 1$. The case $j = 3$ is completely parallel. For $j = 1$, substituting $t_2 = R\exp(\mathrm{i}\theta)$ and $q = \mathrm{i}x$, we see that

$$\begin{aligned}(t_2 + t_2^{-1} - q)^2 - 4 &= (R\exp(\mathrm{i}\theta) + R^{-1}\exp(-\mathrm{i}\theta) - \mathrm{i}x)^2 - 4 \\ &= ((R + R^{-1})\cos\theta + \mathrm{i}((R - R^{-1})\sin\theta - x))^2 - 4.\end{aligned}$$

Therefore,

$$\mathrm{Im}\left((t_2 + t_2^{-1} - q)^2 - 4\right) = 2(R + R^{-1})\cos\theta\left((R - R^{-1})\sin\theta - x\right)$$

and $\mathrm{Im}\left((t_2+t_2^{-1}-q)^2-4\right)\leq 0$ if and only if

$$(R-R^{-1})\sin\theta - x \leq 0.$$

Recall that $p_1 = R\exp(\mathrm{i}\theta_0)$. Since $(R-R^{-1})\sin\theta_0 - x = 0$, we deduce that $(R-R^{-1})\sin\theta - x < 0$ for all $\theta\in[0,\theta_0]$ as desired. □

By virtue of Lemma B.1, we see that

$$\begin{aligned}
&\mathrm{Im}\left(\int_{-\partial a(q)} \iota_{\mathrm{i}\partial/\partial q}\check{\Omega}\right)\\
&=\sum_{j=1}^{3}\mathrm{Im}\left(\int_{\gamma_{1,j}}\frac{1}{\sqrt{(t_2+t_2^{-1}-q)^2-4}}\frac{\mathrm{d}t_2}{t_2}\right)\\
&\geq \mathrm{Im}\left(\int_{\mathcal{C}}\frac{1}{\sqrt{(t_2+t_2^{-1}-q)^2-4}}\frac{\mathrm{d}t_2}{t_2}\right)
\end{aligned}\tag{B.3}$$

where $\mathcal{C}$ is the counterclockwise oriented contour $R\exp(\mathrm{i}\theta)$ with $\theta\in[0,\pi/4]$ for all $|q|$ large. This can be done since $\theta_0>\pi/4$ for all q with $|q|\gg 0$.

The third inequality holds as one can see in the above proof. Notice that

$$\frac{\mathrm{d}t_2}{t_2} = \mathrm{i}\mathrm{d}\theta \text{ on } \mathcal{C}.$$

Thus it suffices to compute the real part of the integrand.

Put $q=\mathrm{i}x$. We can easily compute $p_1 = ((q+2)+\sqrt{q(q+4)})/2$ and

$$\lim_{x\to\infty}\frac{|p_1|}{|q|} = \lim_{x\to\infty}\frac{R}{x} = 1.$$

For $t_2 = R\exp(\mathrm{i}\theta)$, we see that

$$\begin{aligned}
|(t_2+t_2^{-1}-q)^2-4|^2 &= |(R\exp(\mathrm{i}\theta)+R^{-1}\exp(-\mathrm{i}\theta)-q)^2-4|^2\\
&\leq \left(R+R^{-1}+|q|\right)^2+4\\
&\leq \kappa_1|q|^2
\end{aligned}$$

for some constant $\kappa_1>0$ and for all $|q|$ large. On the other hand,

$$\begin{aligned}
(t_2+t_2^{-1}-q)^2-4 &= (R\exp(\mathrm{i}\theta)+R^{-1}\exp(-\mathrm{i}\theta)-\mathrm{i}x)^2-4\\
&= \left[(R+R^{-1})\cos\theta+\mathrm{i}\left((R-R^{-1})\sin\theta-x\right)\right]^2-4.
\end{aligned}$$

Let $\eta = (R+R^{-1})\cos\theta+\mathrm{i}\left((R-R^{-1})\sin\theta-x\right)$. Here we remind the reader that R, and hence η, depends on $x=|q|$. Since $\theta\in[0,\pi/4]$, it follows that $(R-R^{-1})\sin\theta-x<0$. Moreover, there exists a positive constant $C>0$ such that

$$\frac{(R-R^{-1})\sin\theta-x}{(R+R^{-1})\cos\theta} = \frac{R-R^{-1}}{R+R^{-1}}\tan\theta - \frac{x}{(R+R^{-1})\cos\theta}\geq -C\tag{B.4}$$

for all $\theta\in[0,\pi/4]$ and all $|q|\gg 0$.

Our goal is to estimate

$$\mathrm{Re}\left(\frac{1}{\sqrt{\eta^2-4}}\right)=\mathrm{Re}\left(\frac{\overline{\sqrt{\eta^2-4}}}{|\eta^2-4|}\right)=\mathrm{Re}\left(\frac{\sqrt{\eta^2-4}}{|\eta^2-4|}\right).$$

Lemma B.2. *For any $\theta\in[0,\pi/4]$, there exists a constant $\kappa_3>0$ such that*

$$|\eta|\geq\kappa_3 x,\ \textit{for all } x\gg 0.$$

Proof. We can compute

$$\begin{aligned}|\eta|^2&=(R+R^{-1})^2\cos^2\theta+(R-R^{-1})^2\sin^2\theta-2x(R-R^{-1})\sin\theta+x^2\\&=R^2+R^{-2}+2\cos 2\theta-2x(R-R^{-1})\sin\theta+x^2\\&\geq R^2-2xR\sin\theta+x^2\\&\geq R^2-\sqrt{2}xR+x^2.\end{aligned}$$

There exists a constant $\kappa_3>0$ such that

$$|\eta|^2\geq R^2-2xR\sin\theta+x^2\geq\kappa_3 x^2$$

for all $x\gg 0$. □

In particular, the lemma above implies

$$\lim_{x\to\infty}\frac{|\sqrt{\eta^2-4}|}{|\eta|}=\lim_{x\to\infty}\left|\sqrt{\frac{\eta^2-4}{\eta^2}}\right|=1.$$

The first equality holds since η lies in the fourth quadrant. Together with (B.4), it then follows that there exist constants $\kappa_4>0$ and $\kappa_5>0$ such that

$$\mathrm{Re}(\sqrt{\eta^2-4})\geq\kappa_4\,\mathrm{Re}(\eta)\geq\kappa_5|q|$$

for all $x\gg 0$; in other words, we have

$$\mathrm{Re}\left(\frac{1}{\sqrt{\eta^2-4}}\right)=\mathrm{Re}\left(\frac{\sqrt{\eta^2-4}}{|\eta^2-4|}\right)\geq\frac{\kappa_5|q|}{\kappa_1|q|^2}=\frac{\kappa_6}{|q|},\ \kappa_6:=\kappa_5\kappa_1^{-1}$$

for all $x\gg 0$. Thus,

$$\begin{aligned}&\mathrm{Im}\left(\int_{\mathcal{C}}\frac{1}{\sqrt{(t_2+t_2^{-1}-q)^2-4}}\frac{\mathrm{d}t_2}{t_2}\right)\\&=\int_{\mathcal{C}}\mathrm{Re}\left(\frac{1}{\sqrt{(t_2+t_2^{-1}-q)^2-4}}\right)\mathrm{d}\theta\\&\geq\int_{\mathcal{C}}\frac{\kappa_6}{|q|}\mathrm{d}\theta\geq\frac{\kappa}{|q|}\end{aligned}$$

for some constant $\kappa>0$ and for all large $|q|$. This proves (B.1).

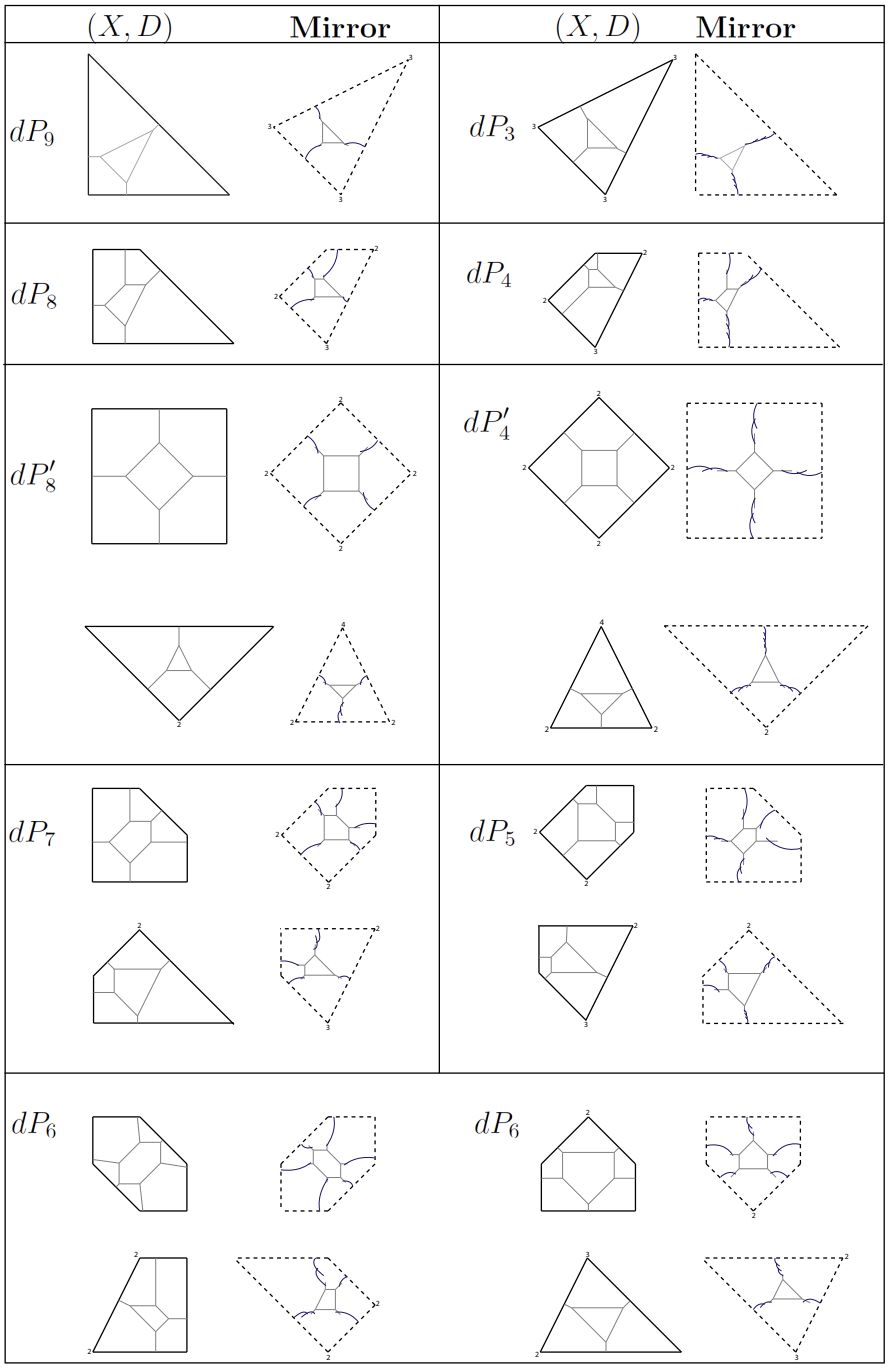

FIGURE 15. Del Pezzo surfaces that come from smoothings of toric Gorenstein surfaces and their mirrors.

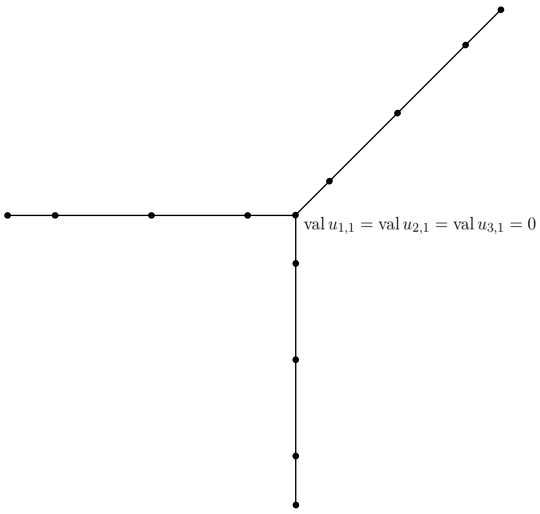

FIGURE 16. A skeleton of mirror of $dP_3 - E$ formed by the valuation image.

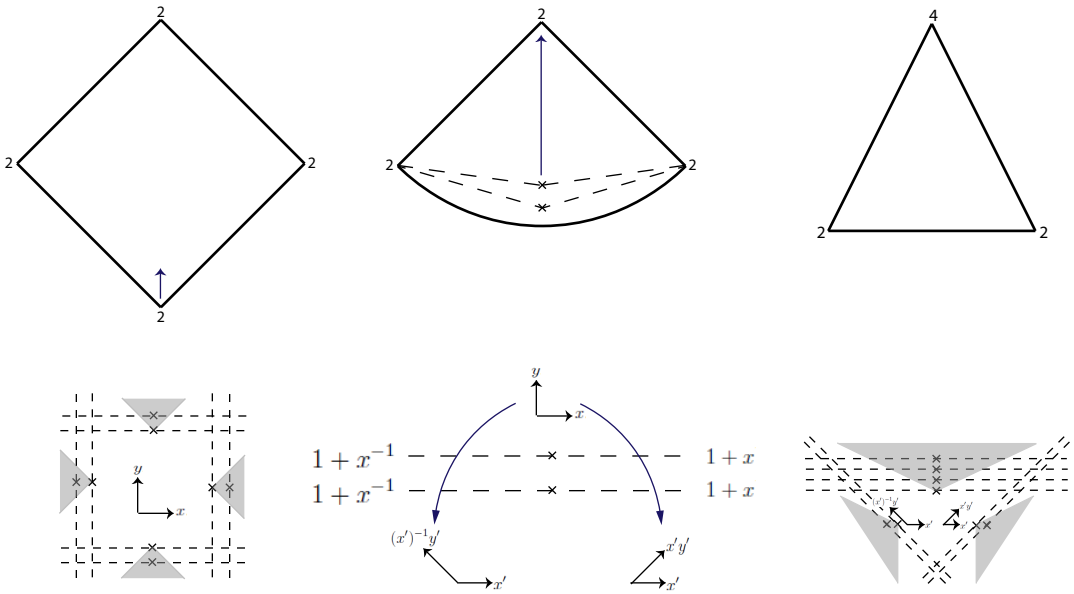

FIGURE 17. Wall crossing for dP_4'.

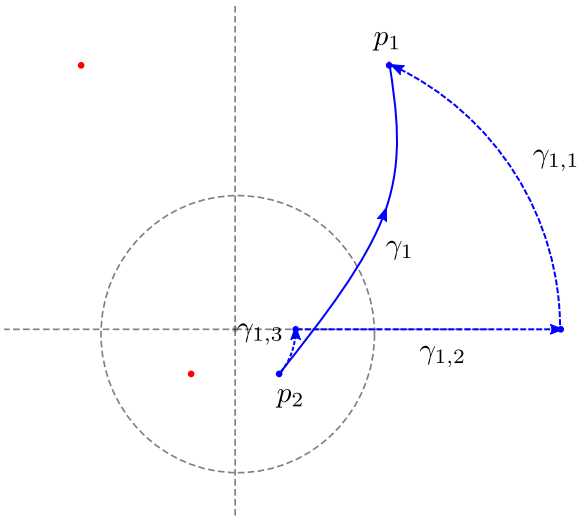

FIGURE 18. p_1 and p_2 are ramification points.

References

[1] M. Abouzaid, *Family Floer cohomology and mirror symmetry*, Proceedings of the International Congress of Mathematicians—Seoul 2014. Vol. II, 2014, pp. 813–836. MR3728639 ↑2

[2] ———, *The family Floer functor is faithful*, J. Eur. Math. Soc. (JEMS) **19** (2017), no. 7, 2139–2217. MR3656481 ↑2

[3] ———, *Homological mirror symmetry without correction*, J. Amer. Math. Soc. **34** (2021), no. 4, 1059–1173. MR4301560 ↑2

[4] M. Akaho and D. Joyce, *Immersed Lagrangian Floer theory*, J. Differential Geom. **86** (2010), no. 3, 381–500. MR2785840 ↑5

[5] D. Auroux, *Mirror symmetry and T-duality in the complement of an anticanonical divisor*, J. Gökova Geom. Topol. GGT **1** (2007), 51–91. MR2386535 ↑3, 6, 32

[6] D. Auroux, L. Katzarkov, and D. Orlov, *Mirror symmetry for del Pezzo surfaces: vanishing cycles and coherent sheaves*, Inventiones Mathematicae **166** (2006), no. 3, 537–582. MR2257391 ↑2

[7] W. P. Barth, K. Hulek, C. A. M. Peters, and A. Van de Ven, *Compact complex surfaces*, Second, Ergebnisse der Mathematik und ihrer Grenzgebiete. 3. Folge. A Series of Modern Surveys in Mathematics [Results in Mathematics and Related Areas. 3rd Series. A Series of Modern Surveys in Mathematics], vol. 4, Springer-Verlag, Berlin, 2004. MR2030225 ↑27

[8] V. V. Batyrev, *Quantum cohomology rings of toric manifolds*, 1993, pp. 9–34. Journées de Géométrie Algébrique d'Orsay (Orsay, 1992). MR1265307 ↑2

[9] M. Carl, M. Pumperla, and B. Siebert, *A tropical view on Landau–Ginzburg models* (2022), available at https://arxiv.org/pdf/2205.07753.pdf. ↑1, 4, 5, 16

[10] K. Chan, *Homological mirror symmetry for A_n-resolutions as a T-duality*, J. Lond. Math. Soc. (2) **87** (2013), no. 1, 204–222. MR3022713 ↑29

[11] M.-W. M. Cheung and Y.-S. Lin, *Some examples of family floer mirrors* (2021), available at 2101.07079. ↑2

[12] C.-H. Cho, H. Hong, and S.-C. Lau, *Gluing localized mirror functors* (2018), available at https://arxiv.org/pdf/1810.02045.pdf. ↑1, 5, 6, 29, 36

[13] C.-H. Cho and Y.-G. Oh, *Floer cohomology and disc instantons of Lagrangian torus fibers in Fano toric manifolds*, Asian J. Math. **10** (2006), no. 4, 773–814. MR2282365 ↑2

[14] T. Coates, A. Corti, S. Galkin, V. Golyshev, and A. Kasprzyk, *Mirror symmetry and Fano manifolds*, European Congress of Mathematics, 2013, pp. 285–300. MR3469127 ↑2

[15] T. Coates, A. Corti, S. Galkin, and A. Kasprzyk, *Quantum periods for 3-dimensional Fano manifolds*, Geom. Topol. **20** (2016), no. 1, 103–256. MR3470714 ↑2

[16] T. C. Collins, A. Jacob, and Y.-S. Lin, *The SYZ mirror symmetry conjecture for del Pezzo surfaces and rational elliptic surfaces* (Dec. 2020), available at https://arxiv.org/pdf/2012.05416v1. ↑3, 4, 5, 15, 26

[17] ———, *Special Lagrangian submanifolds of log Calabi–Yau manifolds*, Duke Math. J. **170** (2021), no. 7, 1291–1375. MR4255060 ↑1, 2, 3, 4, 5, 15, 17

[18] ———, *The Torelli theorem for ALH^* gravitational instantons*, Forum Math. Sigma **10** (2022), Paper No. e79, 11. MR4589525 ↑16

[19] D. A. Cox, J. B. Little, and H. K. Schenck, *Toric varieties*, Graduate Studies in Mathematics, vol. 124, American Mathematical Society, Providence, RI, 2011. MR2810322 ↑10

[20] Y. Eliashberg and L. Polterovich, *The problem of Lagrangian knots in four-manifolds*, Geometric topology (Athens, GA, 1993), 1997, pp. 313–372. ↑39

[21] R. Friedman, *On the geometry of anticanonical pairs* (Feb. 9, 2015), available at https://arxiv.org/pdf/1502.02560v2. ↑9, 12

[22] K. Fukaya, *Floer homology for families—a progress report*, Integrable systems, topology, and physics (Tokyo, 2000), 2002, pp. 33–68. MR1953352 ↑2

[23] K. Fukaya, Y.-G. Oh, H. Ohta, and K. Ono, *Lagrangian intersection Floer theory: anomaly and obstruction. Part I*, AMS/IP Studies in Advanced Mathematics, vol. 46, American Mathematical Society, Providence, RI; International Press, Somerville, MA, 2009. MR2553465 ↑2, 5

[24] ———, *Lagrangian intersection Floer theory: anomaly and obstruction. Part II*, AMS/IP Studies in Advanced Mathematics, vol. 46, American Mathematical Society, Providence, RI; International Press, Somerville, MA, 2009. MR2548482 ↑5
[25] A. B. Givental, *Homological geometry. I. Projective hypersurfaces*, Selecta Math. (N.S.) **1** (1995), no. 2, 325–345. MR1354600 ↑2
[26] ———, *A mirror theorem for toric complete intersections*, Topological field theory, primitive forms and related topics (Kyoto, 1996), 1998, pp. 141–175. MR1653024 ↑2
[27] T. Gräfnitz, H. Ruddat, and E. Zaslow, *The proper Landau–Ginzburg potential is the open mirror map* (202204), available at https://arxiv.org/pdf/2204.12249.pdf. ↑2
[28] Y. Groman and U. Varolgunes, *Locality of relative symplectic cohomology for complete embeddings*, Compos. Math. **159** (2023), no. 12, 2551–2637. MR4653165 ↑2
[29] M. Gross, *Mirror symmetry and the Strominger–Yau–Zaslow conjecture*, Current developments in mathematics 2012, 2013, pp. 133–191. MR3204345 ↑2
[30] M. Gross, P. Hacking, and S. Keel, *Moduli of surfaces with an anti-canonical cycle*, Compos. Math. **151** (2015), no. 2, 265–291. MR3314827 ↑5, 7, 8, 9, 12, 41
[31] M. Gross and B. Siebert, *From real affine geometry to complex geometry*, Ann. of Math. (2) **174** (2011), no. 3, 1301–1428. MR2846484 ↑2
[32] M. Gross, V. Tosatti, and Y. Zhang, *Collapsing of abelian fibered Calabi–Yau manifolds*, Duke Math. J. **162** (2013), no. 3, 517–551. MR3024092 ↑4
[33] M. Gross and P. M. H. Wilson, *Large complex structure limits of K3 surfaces*, Journal of Differential Geometry **55** (2000), no. 3, 475–546. MR1863732 ↑3
[34] M. Gross and P. M. H. Wilson, *Mirror symmetry via 3-tori for a class of Calabi–Yau threefolds*, Math. Ann. **309** (1997), no. 3, 505–531. ↑5
[35] P. Hacking and A. Keating, *Symplectomorphisms of mirrors to log Calabi–Yau surfaces*, arXiv:2112.06797 (2021). ↑6, 16
[36] ———, *Homological mirror symmetry for log Calabi-Yau surfaces*, Geom. Topol. **26** (2022), no. 8, 3747–3833. With an appendix by Wendelin Lutz. MR4562569 ↑5, 7, 9
[37] H.-J. Hein, S. Sun, J. Viaclovsky, and R. Zhang, *Nilpotent structures and collapsing Ricci-flat metrics on the K3 surface*, J. Amer. Math. Soc. **35** (2022), no. 1, 123–209. MR4322391 ↑4
[38] N. J. Hitchin, *The moduli space of special Lagrangian submanifolds*, Ann. Scuola Norm. Sup. Pisa Cl. Sci. (4) **25** (1997), no. 3-4, 503–515 (1998). Dedicated to Ennio De Giorgi. MR1655530 ↑15
[39] S. Honda, S. Sun, and R. Zhang, *A note on the collapsing geometry of hyperkähler four manifolds*, Science China. Mathematics **62** (2019), no. 11, 2195–2210. MR4028269 ↑4
[40] H. Hong, Y. Kim, and S.-C. Lau, *Immersed two-spheres and SYZ with application to Grassmannians*, J. Differential Geom. **125** (2023), no. 3, 427–507. ↑1, 5, 6, 29, 32
[41] H. Hong, Y.-S. Lin, and J. Zhao, *Bulk-deformed potentials for toric Fano surfaces, wall-crossing, and period*, Int. Math. Res. Not. IMRN **16** (2022), 12699–12766. MR4466010 ↑2
[42] K. Hori and C. Vafa, *Mirror Symmetry* (Feb. 2000), available at https:/arxiv.org/pdf/hep-th/0002222v3. ↑2
[43] M. Kontsevich, , Lectures at ENS, Spring, Paris, 1998, notes taken by J. Bellaiche, J.-F. Dat, I. Marin, G. Racinet and H. Randriambololona. ↑2
[44] M. Kontsevich and Y. Soibelman, *Homological mirror symmetry and torus fibrations*, Symplectic geometry and mirror symmetry (Seoul, 2000), 2001, pp. 203–263. MR1882331 ↑3, 4
[45] ———, *Affine structures and non-Archimedean analytic spaces*, The unity of mathematics, 2006, pp. 321–385. MR2181810 ↑2, 17
[46] Vik. S. Kulikov, *Degenerations of K3 surfaces and Enriques surfaces*, Izv. Akad. Nauk SSSR Ser. Mat. **41** (1977), no. 5, 1008–1042, 1199. MR0506296 ↑4
[47] S.-C. Lau, T.-J. Lee, and Y.-S. Lin, *On the complex affine structures of SYZ fibration of del Pezzo surfaces*, Adv. Theor. Math. Phys. **26** (2022), no. 4, 921–955. ↑4
[48] S.-C. Lau, N. C. Leung, and B. Wu, *Mirror maps equal SYZ maps for toric Calabi-Yau surfaces*, Bull. Lond. Math. Soc. **44** (2012), no. 2, 255–270. MR2914605 ↑29

[49] Y. Li, *Strominger–Yau–Zaslow conjecture for Calabi–Yau hypersurfaces in the Fermat family*, Acta Math. **229** (2022), no. 1, 1–53. MR4460593 ↑4
[50] Y.-S. Lin, S. Soundararaja, and X. Zhu, *Non-collapsing degeneration of ALH*-gravitational instantons*, work in progress. ↑4
[51] Y.-S. Lin and R. Takahashi, *Collapsings of* ALH**-gravitational instantons*, preprint 2023, arXiv: 2305.16096. ↑4
[52] R. Miranda, *The basic theory of elliptic surfaces*, Dottorato di Ricerca in Matematica. [Doctorate in Mathematical Research], ETS Editrice, Pisa, 1989. MR1078016 ↑9
[53] R. Miranda and U. Persson, *Mordell–Weil groups of extremal elliptic K3 surfaces*, Problems in the theory of surfaces and their classification (Cortona, 1988), 1991, pp. 167–192. MR1273378 ↑26
[54] Y. Odaka and Y. Oshima, *Collapsing K3 surfaces and Moduli compactification*, Proc. Japan Acad. Ser. A Math. Sci. **94** (2018), no. 8, 81–86. MR3859764 ↑3, 4
[55] H. Ruddat and B. Siebert, *Period integrals from wall structures via tropical cycles, canonical coordinates in mirror symmetry and analyticity of toric degenerations*, Publ. Math. Inst. Hautes Études Sci. **132** (2020), 1–82. ↑5
[56] M. Schütt and T. Shioda, *Elliptic surfaces*, Algebraic geometry in East Asia—Seoul 2008, 2010, pp. 51–160. MR2732092 ↑26
[57] P. Seidel, *Homological mirror symmetry for the genus two curve*, J. Algebraic Geom. **20** (2011), no. 4, 727–769. ↑5
[58] P. Seidel and R. Thomas, *Braid group actions on derived categories of coherent sheaves*, Duke Math. J. **108** (2001), no. 1, 37–108. MR1831820 ↑29
[59] A. Strominger, S.-T. Yau, and E. Zaslow, *Mirror symmetry is T-duality*, Nuclear Phys. B **479** (1996), no. 1-2, 243–259. ↑1, 3
[60] R. P. Thomas, *Stability conditions and the braid group*, Comm. Anal. Geom. **14** (2006), no. 1, 135–161. MR2230573 ↑29
[61] G. Tian and S.-T. Yau, *Complete Kähler manifolds with zero Ricci curvature. I*, J. Amer. Math. Soc. **3** (1990), no. 3, 579–609. MR1040196 ↑3
[62] J. Tu, *On the reconstruction problem in mirror symmetry*, Adv. Math. **256** (2014), 449–478. MR3177298 ↑2
[63] H. Yuan, *Family Floer program and non-archimedean SYZ mirror construction*, preprint 2020, arXiv: 2003.06106. ↑2

Email address: lau@math.bu.edu

Mathematics and Statistics Department, Boston University, 111 Cummington Mall, Boston MA 02215

Email address: tsungju@gs.ncku.edu.tw

Department of Mathematics, National Cheng Kung University, No. 1 Daxue Rd., East District, Tainan 70101, Taiwan

Email address: yslin@bu.edu

Mathematics and Statistics Department, Boston University, 111 Cummington Mall, Boston MA 02215